CR-180811
R87-916527-1

NASA

# HIGH TEMPERATURE STATIC STRAIN GAGE DEVELOPMENT CONTRACT

By
C.O. Hulse, R.S. Bailey, H.P. Grant
and J.S. Przybyszewski

United Technologies Research Center



Prepared for
National Aeronautics and Space Administration

NASA Lewis Research Center
Contract NAS3-23722
July 1987

UNITED
TECHNOLOGIES
RESEARCH
CENTER
East Hartford, Connecticut 06108

# High Temperature Static Strain Gage Development Contract

REPORTED BY 

C. O. Hulse

APPROVED BY 

E. R. Thompson
Assistant Director of Research
for Materials Technology

DATE July 1987

NO. OF PAGES _____

COPY NO. _____

# TABLE OF CONTENTS


| Section | | Page |
|---|---|---|
| 1.0 | SUMMARY | 1 |
| 2.0 | INTRODUCTION | 3 |
| 3.0 | APPROACH | 5 |
| 4.0 | EXPERIMENTAL PROCEDURE | 7 |
| | 4.1 Sample Preparation | 7 |
| | 4.2 Measurements of Electrical Resistance | 9 |
| | 4.3 Stress-Strain and Other Properties | 12 |
| 5.0 | RESULTS | 15 |
| | 5.1 Initial Alloy Evaluation and Selection | 15 |
| | 5.2 Electrical Resistance Properties of FeCrAl Alloys | 16 |
| | 5.3 Electrical Resistance Properties of Cast PdCr Alloys | 17 |
| | 5.4 Mechanical and Other Properties of Cast Materials | 20 |
| | 5.5 Fabrication of Sputtered Samples | 21 |
| | 5.6 Electrical Properties of Sputtered Pd-13Cr | 23 |
| 6.0 | DISCUSSION OF RESULTS | 25 |
| | 6.1 FeCrAl Type Alloys | 25 |
| | 6.2 PdCr Type Alloys | 25 |
| 7.0 | SUMMARY AND CONCLUSIONS | 29 |
| 8.0 | REFERENCES | 31 |

TABLES

FIGURES

# L I S T  O F  T A B L E S


| Table | Title |
|---|---|
| 5.1.1 | Oxidation Results for FeCrAl Alloys |
| 5.1.2 | Results of PdCr Type Alloy Solubility Study |
| 5.1.3 | Oxidation of Cast PdCr Type Alloys |
| 5.2 | Summary of Data for Cast FeCrAl Type Alloys |
| 5.3.1 | Summary Data for Cast PdCr Type Alloys |
| 5.3.2 | Heating and Cooling Reproducibility of Pd-13Cr (Wt %) |
| 5.3.3 | Heating and Cooling Repdoducibility of Pd-22Cr (Wt %) |
| 5.4.1 | Mechanical Properties of Pd-13Cr (Wt %) in Tension |
| 5.4.2 | Chemical Analysis of Arc-Melted Pd-13Cr (Wt %) |
| 5.5.1 | Sputtered Pd-Cr, Fabrication, Parameters and Results |
| 5.5.2 | Summary of Heat Treatment and Results for Sputtered PdCr |

# LIST OF FIGURES


| Figure | Title |
|---|---|
| 4.1.1 | Tri-Arc Melter Showing Position of Splat Cooling Ram and Drop-Casting Tube |
| 4.1.2 | Configuration of Sputtered Strain Gage |
| 4.2.1 | High Speed Thermal Cycle Resistance Measurement Apparatus |
| 5.2.1 | Compositional Variations in Rods Drop Cast for Resistivity Measurements |
| 5.2.2 | Changes in Resistance vs. Temperature of Drop Cast FeCrAl Mod. #3 Rods |
| 5.2.3 | Change in Resistance vs. Temperature of FeCrAl Mod. #3 After Different Soak Times at 1250 K |
| 5.3.1 | Change in Resistance vs. Temperature of Pd-13 wt% Cr at 50 and 250 K/min |
| 5.3.2 | Resistivity and Thermal Coefficient of Resistivity of PdCr Alloys |
| 5.3.3 | Change in Resistance vs. Temperature of PdCr Alloys at 50 K/min |
| 5.3.4 | Change in Resistance vs. Temperature of Pd-18Cr-8Ta (wt%) |
| 5.3.5 | Change in Resistance vs. Temperature of Pd-16Cr-8Ni (wt%) |
| 5.3.6 | Change in Resistance vs. Temperature of Pd-16Cr-10Ni (wt%) |
| 5.3.7 | Change in Resistance vs. Temperature Before and After 10 hour Drift Runs Pd-16Cr-8Co (wt%) |
| 5.3.8 | Drift of Pd-20Cr (wt%) and Pd-13Cr (wt%) at 1250 K |
| 5.3.9 | Resistance Drift of PdCr Alloys in Argon at 1250 K |
| 5.3.10 | Resistance Drift of PdCr Alloys in Air at 1250 K |
| 5.3.11 | Elemental Composition Profiles at the Surface of Pd-13Cr (wt%) Sample After 40 hours in Air at 1250 K |
| 5.3.12 | View of Oxide Surface Film on Pd-13Cr (wt%) |
| 5.3.13 | Change in Resistance vs. Temperature at 50 K/min in Argon of Splat Cast Foil Pd-13 w/o Cr (wt%) |
| 5.3.14 | Drift in Resistance at 1250 K for 50 hours in Air of Splat Cast Foil Pd-13Cr (wt%) |
| 5.4.1 | Thermal Expansion of Pd-13Cr (wt%) in Argon |
| 5.4.2 | Coefficient of Thermal Expansion of Pd-13Cr (wt%) in Argon |
| 5.4.3 | Strength vs. Temperature of Drop Cast Pd-13Cr (wt%) |
| 5.4.4 | Strain-to-Failure vs. Temperature of Drop Cast Pd-13Cr (wt%) |
| 5.4.5 | High Temperature Stress-Strain Curves of Drop Cast Pd-13Cr (wt%) |

## L I S T  O F  F I G U R E S (Concluded)


| Figure | Title |
|---|---|
| 5.4.6 | Variation of Resistance and Stress with Strain at Room Temperature in Pd-13Cr (wt%) |
| 5.4.7 | Effect of Strain Rate on the Gage Factor at Room Temperature of Pd-13Cr (wt%) |
| 5.5.1 | As-Sputtered Pd-13Cr (wt%) on Coated Hast-X |
| 5.5.2 | Holes in Sputtered PdCr Films after Recrystallization |
| 5.5.3 | Edge Protrusions on PdCr Grid After Oxidation of 0.5 μm Al Overcoat (Sample HX-5) |
| 5.6.1 | Resistance vs. Temperature for Sputtered Pd-13Cr (wt%) Pretreated 10 hours in Air at 1370 K |
| 5.6.2 | Change in Resistance vs. Temperature at 50 K/min in Air Pd-13Cr (wt%) After Pretreated 1250 K 10 hours in Air |
| 5.6.3 | Effect of Sample Thickness on Drift in Resistance of Pd-13Cr (wt%) in Air at 1250 K |

## 1.0 SUMMARY

This report describes the results of Tasks 1 and 2 of contract NAS23722 to continue the further development of two high temperature resistive strain gage alloy candidates. The compositions of these two alloys in weight percent were: Fe-10.6Cr-11.9Al and Pd-13Cr. These alloys were to be capable of use as static strain gages on gas turbine blades or vanes inside gas turbine test stand engines at temperatures up to 1250 K. The strain gages were to have lifetimes of at least 50 hours at maximum strain levels of ± 2,000 microstrain with errors of no more than ± 10 percent of full scale. The final gages were to measure no more than 3 mm on a side for use on smaller airfoils, with total gage thicknesses not to exceed 0.5 mm for a wire gage or 0.2 mm for a foil type strain gage.

Twenty-seven samples of different FeCrAl alloys were examined to determine various properties. Most of these samples were prepared as drop cast rods after arc-melting on a cold hearth. Weight loss experiments to measure the effects of additions of Hf, Zr, Y, Co, Ni, and Sc on the oxidation resistance of an alloy of nominal composition Fe-10.6Cr-11.9Al in weight percent did not result in significant improvements in resistance to oxidation at 1250 K. Other experiments with this alloy revealed that continued exposure to air at 1250 K results in a slow shift of the resistivity versus temperature curve toward higher values of resistance at higher temperatures. Primarily because the most important property of the final alloy developed must be stability and repeatability, it was decided to discontinue further work on this alloy system and to concentrate further efforts on the Pd-13 weight percent Cr alloy.

Seventy arc-cast samples and sixteen sputtered samples of PdCr alloys were prepared and examined. These alloys form an adherent, self-protective scale of $Cr_2O_3$ which resists additional oxidation of the remaining Cr which stays in complete solid solution over the full temperature range of interest. Metallographic examinations were conducted and estimates made of the solubilities of Er, Co, Ta, Gd, La, Re, Y, Mo, and W in alloys of nominal composition Pd-13 weight percent Cr. Measurements of the change in the weight of alloys with various additions of these elements failed to reveal any alloys with improved resistances to oxidation, so that the composition of the optimum strain gage alloy remained the same as originally developed, Pt-13 weight percent Cr.

The yield strength and strain to failure of the well-annealed alloy varied from 123 MPa and 26.9% at room temperature to 8.5 MPa and 14.5% at 1250 K in air. This alloy had a room temperature gage factor of 1.78. This factor appeared to vary with strain after plastic yielding but this may have been because the commercial strain gage being used was similar in size to the grains present in the test material.

Although the stability of electrical resistance of this alloy at 1250 K in air was good when the material was in bulk form, oxidation studies of splat-cooled foils indicated that the amount of drift in electrical resistance at 1250 K is strongly influenced by the surface to volume ratio and any failures in the oxide scale. The total apparent strain drift of a 6 μm (micrometer) thick sputtered film of this alloy over a 50 hour period in air at 1250 K was about 12,000 μstrain. Unsuccessful attempts were made to prevent oxidation attack of these very thin sputtered films by applying sputtered overcoats of Al which were subsequently oxidized to form $Al_2O_3$. New impervious overcoats will need to be developed in subsequent tasks in order to proceed with the complete development of useful strain gage systems. In addition, a dual element, thermally compensated gage design will also need to be developed because of the relatively high thermal sensitivity of the resistance of this alloy.

## 2.0 INTRODUCTION

Continued advances in the development of more efficient and higher specific thrust gas turbine engines depend upon the utilization of improved designs and materials. The continued development of sophisticated computers and advances in fluid mechanics, thermal analysis, aerodynamics and aeromechanic modeling means that detailed analysis and estimations can be made of the conditions inside operating gas turbine engines. The use of these calculations and models to develop improved designs requires accurate, specific experimental data about the behavior of engine parts during operation in order to establish their validity. The local strain behavior at various points is one of the most significant and yet difficult kinds of real time data required for these purposes.

The purpose of this program is to develop a new resistive strain gage alloy and a complete measurement system which can operate inside gas turbines running on test stands. The specific program goals are to develop a static gage system capable of at least 50 hours of operation at temperatures up to 1250 K (1800°F) on a vane or rotating gas turbine blade. The surface dimensions of the gage are limited to 3 mm x 3mm. The maximum height above the airfoil must be less than 0.2 mm for a foil gage and 0.5 mm for a wire gage. The desired maximum strain capability is ± 2,000 μstrain (.2 percent strain) at 1250 K and ± 3,000 μstrain at 1100 K with an inaccuracy of no more than ± 10% of the full scale reading. This program is part of a much larger NASA effort, the HOST Program, to develop improved HOT Section Technology for gas turbine engines.

Dynamic strain gages have been developed which, although they do not meet the above size restrictions, can operate up to 1250 K inside a gas turbine engine. The measurement of strain is greatly simplified in the dynamic case because the intent is only to compare the maximum and minimum strains created almost instantaneously by vibratory stresses. Static strain gages are required to operate accurately over long periods of time at various temperatures without significant drift or error. The best alloys currently available are the Ni-Cr alloys and variations of FeCrAl alloys which are all sensitive to the rates of heating and cooling at lower temperatures. With very careful calibration, a FeCrAl alloy has been used to make static strain measurements to approximately 980 K (Ref. 1).

The fact that the resistances of these alloys show nonlinear behavior with temperature is an indication that internal microstructural changes are taking place. It is believed that these effects are caused by various types of ordering reactions. Although these changes are relatively rapid, they still have time dependent features, which explains why the resistance versus time curves of these materials vary with the rates of heating and cooling.

The directions of these nonlinearities are to make the resistances of these materials relatively insensitive to temperature change. This is important to our application because the temperatures of materials inside jet engines are not well known. Current estimates of typical errors are about 10 K. Errors in temperature translate directly into uncertainties in the correct value of strain. The larger the value of the thermal coefficient of resistivity of the sensor alloy, the greater will be the error in strain which results from our inability to make accurate measurements of the temperature.

In addition to metallurgical and chemical stability, especially with respect to oxidation, an important property of the resistive sensor alloy is that it have a low value of alpha, the thermal coefficient of resistance. Although pure metals, especially precious metals, can be very stable and inert, they all have high values of alpha. We must therefore examine the potential of metal alloys to find usable strain sensitive resistors. This search was the subject of a prior contract effort (Refs. 2-4). It was concluded in those efforts that attention should concentrate on phase pure alloys. The relative solubilities of phases in each other will change with temperature and with time at temperature, so that serious problems with electrical drift can be expected in multiphase systems. The problem reduces to finding chemically inert alloys, particularly with respect to oxidation, which have high concentrations of other elements which will remain in complete solid solution over the full range of temperatures to be encountered.

Two alloys were selected as the result of the prior effort referenced above: Palladium containing 13 weight percent Cr and the FeCrAl alloy, Fe-10.6Cr-11.9Cr, also in weight percent. The primary subject of this report is to describe the further efforts made to more fully optimize and characterize these alloys and to study how they could be fabricated into resistive strain sensors. This report is a progress report on the alloy development phases of a larger contract program in which a complete strain gage system using the new, higher temperature alloy will be fabricated and evaluated.

This program was conducted as a joint effort by the Research Center and the Pratt and Whitney Aircraft Division. Howard Grant served as the Principal Investigator at Pratt and Whitney with John Przybyszewski to complete their part of the program.

## 3.0 APPROACH

The approach used in Tasks 1 and 2 of this program was to continue using the ideas and experimental procedures developed in the previous contract, (Ref. 2), to develop a static strain gage alloy which would be useful to 1250 K. Task 1 consisted of an iterative program to further modify the compositions of the two alloys developed in the above contract:

Pd - 13% Cr
Fe - 1.06% Cr - 11.9% Al,

where the percentages are in weight percent. These samples were to be studied with the dual objectives of improving their resistances to oxidation and also lowering their thermal coefficients of resistance without adversely affecting the repeatability of the thermal coefficient of resistance. The new alloy modifications were to be prepared by arc melting and drop casting into fused silica tubes to produce sample rods for further evaluations, as before.

Improvements in the resistance to oxidation from additions of various alloying elements to a series of cast rods were to be evaluated by making measurements of their relative changes in weight and by measuring the depths of alloy composition variation under oxide surface films after long term exposures to air at 1250 K. It was subsequently realized that this was a relatively coarse measurement approach for our purposes. Measurement of electrical resistance is a more sensitive and direct technique for this evaluation as became apparent during the subsequent thermal cycling and electrical resistance drift testing portions of the program.

Measurements of the thermal coefficient of resistance (alpha), reproducibility of resistance, and stability with time were made using an electrical resistance measuring facility developed during the previous contract. The sensitivities to thermal rate effects were similarly evaluated by heating and cooling at 50 and 250 K/min. Final evaluations of the stability of resistivity with time of the best alloys were evaluated by 50 hour drift experiments in air at constant temperatures of 1100 and 1250 K.

Additional measurements were also to be made to determine the sensitivities of the best PdCr and FeCrAl alloys to changes in composition. The intention was to evaluate to what degree the composition had to be controlled in order to obtain the optimum properties. The final effort in Task 1 was to determine a number of other properties of the best alloys. These properties were to include composition, stress-strain characteristics over the temperature range of interest, the coefficient of thermal expansion and the strain gage factor at room temperature.

Task 2 was primarily concerned with an examination of gage fabrication techniques. Sputtering was the main technique to be examined because of prior successful development experience and because it could also be used to form a high quality, well-bonded electrically insulating subcoating between the sensor and the substrate.

The original plan to examine the behavior of the sputtered alloy on a dense alumina substrate was changed to an examination of the sputtered alloy on a Hastelloy X substrate with a sputtered insulation layer of aluminum oxide in between. This change was made to better duplicate the conditions present in an actual installation, especially as regards the strains resulting from differential thermal expansion forces which would necessarily be present. Each sample was to be examined for proper composition, uniformity of composition, and oxidation resistance (50 hours in air at 1250 K). The repeatibility of both resistivity and the thermal coefficient of resistance over the temperature range from 300 to 1250 K was to be evaluated both before and after oxidation testing. The oxidation resistance and the stability of resistance with time (50 hours at 1250 K) were also to be determined. At the conclusion of these tests, UTRC was to recommend the best method of fabrication for each type of alloy.

The approach used in the selection of alloying elements for improved oxidation was to draw upon corporate knowledge and the experience of others. Minor alloying additions were made which had been shown (Refs. 5-7) to significantly improve the oxidation behavior of nickel-base superalloys. The oxidation resistances of these materials depend primarily upon the formation of coatings of $Cr_2O_3$ and $Al_2O_3$, which are isomorphous with each other.

The alloying guide line from the prior program that all alloying elements must be in complete solid solution over the entire temperature range of use was continued in this program. If any second phases were permitted to be present in the final alloy, it would be expected that their solubilities, and therefore the concentration of solute electron scattering centers, would vary with temperature and time-temperature history which would result in an unstable, nonreproducible resistor alloy.

# 4.0 EXPERIMENTAL PROCEDURE

## 4.1 Sample Preparation

Arc-melting on a water-cooled, cold copper hearth was selected as the best method for preparing contamination free alloy samples. This approach had been developed and used in the prior NASA contract. A commercial* three electrode melter with tungsten electrodes was used with an atmosphere of gettered argon over the sample. The oxygen content of the argon after it had passed through the melting chamber, as measured by an oxygen analyzer incorporated in the titanium gettering system**, was typically less than $10^{-7}$ ppm.

The initial elemental components all had purities of at least 99.9 weight percent. In the case of palladium, the initial material was finely divided sponge so that some material could have been lost during the initial contact with the arc. This material was partially premelted to ensure that the batch composition would agree with the desired composition of the final alloy. The alloy buttons were typically turned over and remelted three times to insure uniform mixing.

In order to prepare test samples as round rods by drop casting, the flat water-cooled copper hearth in the arc melter was replaced by another hearth with a vertical, centered hole as shown in Figure 4.1.1. The alloy button, with the bottom surface polished flat, was placed over the hole and melted again. When the bottom of the button which was against the water-cooled hearth melted, the small argon over-pressure in the melting chamber became sufficient to blow the melt into the hole where it immediately solidified as a rod. The casting hole contained a fused silica tube which started just below the surface of the hearth and received the melted metal. Because of the smoothness of the inside surfaces of the fused silica tubes and its low coefficient of thermal expansion, the test samples normally slid freely out of the silica tubes. Typically cast samples were from 8 to 18 cm long and 0.200 cm in diameter.

Samples of PdCr for metallographic examinations of the solubilities of various elements were prepared as arc melted buttons. These normally weighed about 10 grams and typically were remelted three times. These buttons were subsequently stabilized and homogenized by soaking for 3 hrs at 1470 K, cooled to 1270 K in about 1 hour, and then slow cooled to 770 K at about 25 K/Hr in tank argon (typically 1 to 2 ppm oxygen). During these heat treatments, the samples were held inside individual pure alumina tubes which were wrapped with tantalum foils to getter any traces of oxygen or water vapor which might have been present.

*,**Centorr Associates, Suncook, N.H.

Samples for oxidation tests on FeCrAl and PdCr alloys were prepared as rods by drop casting inside fused silica tubes. After casting, the FeCrAl rods were soaked for 24 hrs at 1570 K in argon in order to homogenize the microstructure. Before testing, the PdCr rods were soaked for 2 hrs in argon at 1470 K. During these treatments, both types of samples were held inside individual alumina tubes which were wrapped in tantalum foils. After these heat treatments, the samples were all lightly polished using 600 grit paper and rinsed in alcohol. The PdCr sample for thermal expansion testing was prepared in the same manner as described above except that after heat treatment it was cut to 2.5 cm in length with squared ends.

Samples for resistance measurements were prepared from drop cast rods which were subsequently reduced by grinding and polishing to thin strips. A special hardened steel plate containing flat bottomed slots of different depths was prepared in order to accomplish this task. The rods were cemented into one of these slots with a thermal wax (bee's wax plus rosin) and then the plate was manually held on a polishing wheel until all of the material which protruded above the slot was removed in a uniform fashion. In order to avoid the presence of any of the small shrinkage voids which were sometimes present at the centers of the rods, the sample strip was normally taken slightly off center from the center of the original cast rod. Typical final dimensions were .056 x .20 cm in cross-section and 11.5 cm in length.

Samples for tensile testing were prepared by clamping and waxing the cast cylindrical rods on a flat plate and milling away a reduced section in the center third of the sample rod. In order to prepare a symmetrical sample, the rod had to be turned over, recemented, and milled again in order to form an approximately centered gage section, typically 0.056 cm thick and as wide as the original diameter of the cast rod. Before testing, these samples were heated for 2 hours in argon at 1470 K to homogenize their chemical composition and to produce an annealed sample with a stable grain structure. For these treatments, the samples were held inside small alumina tubes which were wrapped in tantalum foils in order to getter away any oxygen or water vapor which might have been present.

Samples for measurements of the electrical resistance properties of FeCrAl and PdCr alloys were also prepared by splat cooling. In this technique, the flat-bottomed copper plunger shown in Fig. 4.1.1 was dropped down through the center of the three arcs, causing the molten alloy button to be suddenly quenched into a thin flat disk. The bottom flat anvil or hearth was subsequently modified to contain a centered 2.22 cm depression 0.010 cm deep. An additional depression 0.419 cm in diameter and 0.050 cm deep was also added at the center of the first depression. The smaller center depression acted as a collector of any scale on the molten button and helped to keep the molten button centered under the anvil.

The melt buttons used in the fabrication of splat cooling films typically weighed .5 to .7 gm. These were cut from larger triple-melted buttons which normally weighed about 15 gms. The resulting films were approximately .010 to .015 cm thick and 2.5 cm in diameter with a irregular outline. Sample strips 0.28 cm wide were cut as close to the center of the disk as possible and still avoid the thicker center caused by the central depression in the hearth. These strips were then mounted on glass slides and thinned by mechanical polishing down to .008 cm. Both surfaces were mechanically polished through 600 grit paper. In addition testing, another sample was prepared which had been thinned down to .05 mm (50 μm). This sample was electro-discharge machined (EDM) with a special tool so that there would be a section of reduced width in the middle of test section of the sample. The end tabs were .5 cm wide while the reduced section, which was about .70 cm long, was only .30 cm wide.

Test films of approximately Pd-13 weight percent Cr were also prepared by the sputtering technique at Pratt and Whitney Division, East Hartford, Ct. These films were deposited on Hastelloy-X substrates which were .178 cm thick and either 1.5 x 1.9 cm or 1.9 x 8.0 cm in surface dimensions. Prior to this deposition, the surfaces of the substrate were coated with a "ductile" layer of NiCoCrAlY which was subsequentially oxidized and then coated with an additional sputtered alumina insulation layer using procedures developed on a previous contract (ref. 8). Before the alumina layer was grown, the surface of the substrate was polished down to about a 3-5 μin finish. The final grown alumina insulation layer was approximately 1.5 μm thick and covered by a sputtered alumina layer which was also about 1.5 μm thick.

Rectangular test patches were sputtered on the smaller size substrates and a resistor grid pattern suitable for testing in the thermally cycling rig at the Research Center was sputtered on the larger substrates. The dimensions of the commercially prepared masks used to prepare the photo-etched resistor pattern are shown in figure 4.1.2. A commercial sputtering unit was used to prepare these films with target to sample distances of from 6 to 9 cm and 900 to 1100 volts. The target of nominal composition Pd-14 weight percent Cr was 15.2 cm in diameter and 0.20 cm thick. An additional 1 percent of Cr was added to the target composition in an attempt to compensate for Cr which might be lost by oxidation of the sputtered film. The target was commercially prepared by hot pressing prealloyed powders.

### 4.2 Measurements of Electrical Resistance

Electrical resistance measurements were made using a resistively heated tube furnace developed during a prior contract (ref. 2). A diagram of this facility is shown in figure 4.2.1. This facility was all contained inside a large plexiglas box which could be purged with argon to reduce oxidation of the sample.

The 2.5 cm I.D. Inconel heater tube shown in figure 4.2.1 had a total length of approximately 30 cm and was split in half lengthwise to facilitate sample installation. The ends of the heater tube were clamped in water-cooled electrodes which could provide up to 900 Amps. of AC power. The electrode at one end of the furnace was supported by a ball bearing system which prevented mechanical loads from being applied to the tube as it expanded and contracted thermally during use. Power to the furnace was controlled by a commercial controller* and programmer**. The programmer was adjusted to provide for constant temperature soaks at elevated temperatures and/or linear heating and cooling cycles at 50 and 250 K/min.

Alloy sample strips were normally about 7 cm long and had pieces of other sample strips spot welded to each end to form a final sample which was about 20 cm long. The additional length was added to minimize the presence of temperature gradients in the sample during high speed heating and cooling experiments. At 250 K/min, the (maximum) temperature difference between the center and one of the spot welded platinum electrical measurement contacts was 8 K. During isothermal drift experiments at 1250 K the maximum temperature differences measured between one end and the center of the sample did not exceed 1.5 K.

A set of B-1900 superalloy clamping bars which extended 5 cm into each end of the furnace provided good electrical contacts and physical support of the sample. Forcing these two parallel clamping bars together until they touched at their center using a bolt located just outside of the furnace created a clamping force on the end of the sample of at least 100 Newtons over the range of temperatures from ambient to 1250 K, without at any temperature exceedding the yield point of the B-1900. The set of clamping bars at one end of the furnace was supported on alumina rollers to both provide electrical insulation from ground and to avoid applying any appreciable stresses to the samples due to their thermal expansions and contractions which might influence the values the resistances measured.

The four-point measurement technique was used to measure the electrical resistance of the samples. The two probes which measured the voltage drop across the sample were normally 3.8 cm apart and symmetrically located in the middle of the furnace. The two .05 mm diameter platinum lead wires were spot welded directly to the sample.

The temperature of the sample was measured by a .125 mm Pt-Pt10 percent Rh thermocouple whose bead (junction) was spot welded to the sample at the center of the furance. The Pt-Pt10 percent Rh thermocouple that was used to control the furnace was wired to the sample so that the bead pressed against the sample at the center of the furnace.

---

* Model 63911 Process Controller, Research Incorp., Minneapolis, Minn.
** 73211 Data Track Programmer

In order to improve the linearity of furnace control at low temperatures, a muffle made of stainless steel sheet stock was added around the outside of the heater tube. At low temperatures, this was automatically purged with flowing argon to cool the furnace components down fast enough so that proper furnace control could be secured by applying power to the furnace. A layer of fibrous ceramic insulation was also wired around the outside of this muffle. This extra insulation allowed the furnace system to maintain a linear rate of heating at 250 K/min up to within 20 K of the top temperature of interest, 1250 K. The added muffle and the extra insulation are not shown in figure 4.2.1.

A computer*, programmable voltmeter and power supply, and a scanner were used to measure the resistance data and to record it on a floppy disk. The standard accuracy of the voltmeter was 20 μV/V (.002% error) which could be further improved to 4μV/V (.0004% error) by averaging at least five separate readings. A set of measurements was triggered by a sample thermocouple EMF change equivalent to about ± 75 K or, if this did not occur, by the passage of ten minutes (drift testing). The following sequence of measurements were made by the computer in order to determine one electrical resistance data point.

1. Measure sample temperature
2. Voltage across the sample
3. Voltage across precision resistor
4. Repeat reading 2 and 3 for a total of five readings each
5. Measure sample temperature
6. Repeat readings 2 and 3 with power off for a total of five readings each

Allowing slightly more than the time necessary for voltage "settling" after each reading, a full set of the 12 measurements with the power on required about 2.3 seconds to complete.

Using average values from repeated measurements of the same type permitted the determination of the values of a number of variables at the same instant of time and tended to reduce the "noise" in the data. Measurements of the voltage drop across the precision resistor** in series with the sample were used to accurately determine the current through the sample. This precision resistor was separately mounted on a water-cooled plate away from the furnace.

Voltage measurements with no power through the sample were used to reduce any influence on the data of thermocouple effects due to the use of wires with different compositions in the measurement circuit. Typical currents and voltages through and across the sample were .1 to .3 volts and 2.0 Amps. Room temperature experiments established that, at this current level, there were no

*Model 9826, Hewlett Packard
**Model RH-50, Dale Electronics, Columbus, NE

effects on the resistance measurements due to sample heating. The programmable power supply only put current through the sample when a set of measurements was being made. The accuracy of the overall resistance measurement system was estimated to be ± 8 μΩ/Ω excluding any error due to temperature gradients in the sample. Since during heating at 250 K/min the average temperature deviated from the measured midpoint temperature by a maximum of 4 K, this effect could give rise to an error of 680 μΩ/Ω for Pd-13Cr. During isothermal testing, the gradients in the sample were greatly reduced and remained fairly constant throughout the test resulting in a possible error in apparent drift of ± 20 μΩ/Ω.

### 4.3 Stress-Strain and Other Properties

Tensile stress-strain curves of drop cast rods were determined up to 1250 K in air using a resistively heated furnace and a four-screw Tinius Olsen testing machine. Test samples were .2 cm in diameter and approximately 15 cm long. Flat sections were prepared at each end of the sample by grinding away opposite surfaces to provide better contact surfaces with the wedges in the superalloy grips.*

Strain measurements at room temperatures were obtained using commercial strain gages on opposite sides of the samples. A clamp-on extensometer of UTRC design was used to measure strains in tests at temperatures up to 1100 K. The two extensometer parts that clamped to the sample were made out of B-1900 nickel-base superalloy set for a gage length of 5.1 cm. Four alumina rods hung down from these two clamps and the strain was determined from the differential outputs of two LVDT's** attached to these rods below the furnace so as to be electrically in series. In tests above 1100 K, strains were estimated from crosshead motion using the length of the reduced sample section, which was about 5.5 cm, as the gage length.

Thermal expansion measurements on .2 cm Dia. x 2.5 cm long samples were made using a dual tube, all fused quartz dilatometer system similar in design to that described in ASTM E228-71. Thermal expansion data from an LVDT system mounted above the furnace was continuously measured by a computer/voltmeter/scanner system and recorded on a floppy disk. Calculations and plotting of the data in final form, which included comparisons with the data obtained using pure platinum as a calibration sample***, was accomplished using a computer and digital plotter.

Scanning electron microscope (SEM)**** pictures were made of selected samples after first overcoating the samples with about 500 Å of carbon in

---

*Series 4053 Grips, MAR-M246, Applied Test Systems, Saxonburg, Pa.
**Linear Voltage Differential Transformers, Schaevitz Corp., Camden, NJ
***National Bureau of Stds., Washington, DC
****JSM-35, JEOL Ltd., Tokyo, Japan

order to avoid electrical charging effects. An electron microprobe* was also used to obtain detailed information on local area chemical compositions and how this varied across the sample. Standard chemical analysis techniques were used to determine the compositions of various bulk samples.

*Model MBX, Camberra Corp., with Tracor Northern 2000 Energy Dispersive Spectrometer

# 5.0 RESULTS

## 5.1 Initial Alloy Evaluation and Selection

As required by the Statement of Work, the primary evaluation method for the selection of the best alloys for use as strain gage candidates was to be based on obtaining good resistances to oxidation. The specific criteria chosen for optimum behavior was the minimum amount of weight change shown after a 50 hour exposure to air at 1250 K.

A total of 12 FeCrAl alloy samples were prepared by drop casting and oxidized as described in Section 4.0. The base alloy for comparison was the FeCrAl Mod #3 composition, Fe-11.9Al-10.6Cr in Wt.%. Eight of the other alloy compositions contained small additions of rare earth elements selected on the basis of good results reported when they were used as additives to nickel-base superalloy oxide coatings. Another modification (alloy #2) consisted of exposing the base alloy to a preoxidizing treatment of 2 hours at 1370 K with the intention of forming an alpha-alumina coating rather than a gamma alumina coating on the alloy. Another sample (alloy #3) was prepared in an attempt to see if changing the crystal structure of the Fe would cause any useful changes in behavior. Other candidates (alloys #4 and 5) were selected to be on chromium rich and aluminum rich edges of the zero average thermal coefficient of resistivity regions described in work under the prior contract.

The results obtained from the oxidation studies are presented in Table 5.1.1 with the alloys listed by order of rank, with those that showed the least weight change listed first. The best alloy based on this method of comparison was the Mod #3 alloy, the base alloy developed on the prior contract work.

A total of 34 PdCr type alloy samples were prepared by repeatedly melting small 10 gram batches of material together into small buttons. These were subjected to homogenizing and slow cooling heat treatments to determine if any second phases could be formed in alloys of these compositions. Only sample compositions which were apparently single phase were of interest in this program. Table 5.1.2 shows the various compositions prepared and the results of metallographic examinations of sections which had been polished and etched.

The results from the oxidation testing of seven different PdCr type compositions are presented in Table 5.1.3. Alloys containing more than 13 weight percent Cr did not appear to have better resistance to oxidation than the 13 Wt. percent alloy. Alloys containing refractory metal additions, which might be expected to show lower thermal coefficients of resistance also showed considerable gains in weight. The best alloy for further study based on these results was Pd-13 Wt. percent Cr, the optimum alloy identified during the prior contract.

## 5.2 Electrical Resistance Properties of FeCrAl Alloys

Based on the results of the oxidation study, it was decided to examine further the properties of the original base alloy because none of the modified compositions appeared to improve the resistance to oxidation. A total of ten samples of the Mod #3 composition were prepared and their electrical behaviors determined in order to examine the reproducibility of this alloy. These results were also compared in this program with the electrical behavior of the K-5 sample of the same nominal composition prepared in the previous program. These electrical resistivity results are summarized in Table 5.2.

Electron microprobe analysis of sample K-5 revealed its composition to be Fe-12.3 Cr, 9.41 Al in weight percent instead of Fe-10.6 Cr, 11.9 Al specified when casting the sample. Two additional samples, K-Mod 3-1 and K Mod 3-2, were drop cast from the elements in an attempt to produce resistivity samples closer to the specified composition. The composition of these samples varied from each other and from the specified composition as shown in Table 5.2. This variation was thought to be due in part to the very small amounts of material being used for the casting batch (Typically 15 gm). In an attempt to overcome this problem, additional samples were then prepared from 1.3 cm diameter chill cast bars cast from 300 gm melts using another facility. Because of its low thermal coefficient of resistance, these compositions were selected to be close to that of the K-5 composition. The variations in composition between these various compositions are shown on a ternary plot in Figure 5.2.1.

A comparison showing the importance of these relatively small variations in composition on the electrical behavior of this FeCrAl type alloy is presented in figure 5.2.2. The shapes of the resistivity versus temperature curves vary significantly depending on the particular compositions obtained.

In addition to the sensitivity to composition, further work revealed that FeCrAl alloys tend to show gradual changes in their apparent strain versus temperture curves after prolonged exposures to air at 1250 K. Figure 5.2.3 shows a summary of the effect in the form of a series of thermal cycle curves after various soak times at 1250 K in air. Similar results were also obtained with the K-5 alloy. These gradual increases in resistivity may be due to oxidation which is slowly reducing the total amount of electrically conducting material present. These effects might be avoided if the surfaces were sealed in some way so that oxygen could not react with the alloy. Experiments of this type were never performed because it was decided, based on these results, that further work on this alloy should be discontinued and that additional efforts should be focused on the PdCr type alloy.

Although it had the poorest resistance to oxidation of all of the FeCrAl alloys, the only other alloy besides the Mod #3 alloy that was tested for

resistivity and for temperature coefficient of resistance was alloy #3 (Fe-38Ni-20Cr-4Al). This particular alloy modification was selected for examination in order to determine the effects of changing the crystal structure from body centered cubic to face centered cubic by the appropriate substitution of nickel for iron. Although the expected change in structure was not verified by X-ray examination, it was concluded that this alloy was not of further interest because of its high thermal coefficient of resistance (380 μΩ/Ω/K).

## 5.3 Electrical Resistance Properties of Cast PdCr Alloys

Eleven palladium base alloys were chosen for resistance testing based on previous metallographic examinations and evaluations of their resistances to oxidation. A summary of the resistivity data obtained for these alloys is presented in Table 5.3.1.

The reason for the drop in thermal coefficient of resistance of sample PdCr-12-1 listed in Table 5.3.1 from 168.4 μΩ/Ω/K prior to soaking at 1250 K to 160.6 μΩ/Ω/K after soaking at 1250 K is not known. This sample was subsequently soaked at 1250 K for 100 hours with no further significant change in its thermal coefficient of resistance (160.6 to 162). One possible explanation is that the sample was not fully homogenized after the 1470 K homogenizing heat treatment. The sample experienced a high rate of drift at the start of the 1250 K drift (-116 μΩ/Ω/Hr) which slowed dramatically after 4 hours and stabilized at -19 μΩ/Ω/Hr for the remaining 6 hours. A duplicate sample (PdCr-12-2) did not show any change in thermal coefficient of resistance due to soaking at 1250 K.

Seven alloys were tested at both 50 K/min and 250 K/min to evaluate the effects of heating rate on the thermal coefficient of resistance. As shown in Table 5.3.1, only the alloys containing Ta additions were significantly effected by changes in heating rate. Figure 5.3.1 shows a plot of $\Delta R/R$ vs temperature for Pd-13 Cr heated at two rates which is representative of the curves obtained for all the binary PdCr alloys.

For the binary PdCr alloys, the thermal coefficient of resistance decreased with increasing Cr content from a maximum of 168 μΩ/Ω/K for 13 Wt. percent Cr to a minimum of 125 μΩ/Ω/K at 22 Wt. percent Cr. A plot of the thermal coefficient of resistance vs Cr content for these alloys is shown in figure 5.3.2. The resistivity of the binary alloys increased with increasing Cr content from a minimum of 87 μΩ-cm for 12 Wt. percent Cr to a maximum of 136 μΩ-cm for 22 Wt. percent Cr. This data is also plotted in figure 5.3.2. The differences in the thermal coefficients of resistance and resistivity between duplicate samples of the same alloy may be due in part to compositional differences in the samples resulting from losses during the casting of

the small melt pads. Differences in resistivity may also be due to the irregular cross-section of the test samples. Voids created in the drop cast rods during solidification were included in some samples.

Plots of $\Delta R/R$ vs temperature for Pd-13Cr and Pd-22Cr in Wt. percent heated at 50 K/min are presented in figure 5.3.3. Both curves are essentially linear with a slight break at 850 K for Pd-22 Cr and at 950 K for the Pd-13Cr in Wt. percent. These departures from linearity are probably caused by changes in solute solubilities at the temperature where these breaks are observed.

As shown in Table 5.3.2, resistivity tests were also run on several ternary PdCr alloys. The two alloys containing Mo exhibited high drift rates and an appreciable change in the thermal coefficient of resistance after a 10 hour soak at 1250 K. The alloy containing Er had a very high thermal coefficient of resistance. The alloys containing Ta were non-linear with breaks in their resistivity curves at 350 K and 1000 K. Figure 5.3.4 shows this break for Pd-16Cr-8Ta. Again the nonlinear effects are probably associated with changes in solubilities of the constituents at different temperatures. As discussed in the Approach (Section 3.0), these effects were undesirable and cause for dropping these alloys from further consideration.

The alloys containing Ni and Co showed the most promise of the ternary alloys investigated. All three alloys had temperature coefficients of resistance similar to Pd-13Cr, fairly linear resistivity curves and low drift rates at 1250 K. Figures 5.3.5 thru 5.3.7 show resistivity curves for these alloys at 50 K/min in argon. None of these alloys, however, appeared to offer any advantage over Pd-13Cr. Although an addition of 8 weight percent Ni appeared to result in a small improvement in the oxidation resistance of a higher chromium content alloy (see Table 5.1.3), the data did not suggest that it would be better than Pd-13Cr.

All of the binary alloys were tested for stability in argon at 1100 K and at 1250 K by recording $\Delta R/R$ vs time while the samples were soaked for 10 hours at these temperatures. The results of this testing are given in Table 5.3.1. All of these alloys appeared to be stable at 1100 K with total drifts of 200 to 300 $\mu\Omega/\Omega$ (100 to 150 microstrain assuming a gage factor of 2.0). At 1250 K the most stable alloy was Pd-13Cr in Wt. percent, with total drifts of -150 and -680 $\mu\Omega/\Omega$ for duplicate samples. All of the other binary alloys exhibited positive drift which increased with increasing chromium content to a maximum of 3,890 $\mu\Omega/\Omega$ for Pd-22Cr in Wt. percent.

The atmosphere in the resistivity apparatus used for this testing must have contained some oxygen from the purging argon and from the outgassing of the fiberous insulation. In order to determine if the drift at 1250 K was caused by removal of chromium from the alloys by oxidation, the test plan was

modified to include oxidizing each sample in air at 1250 K to form an oxide coating prior to testing in air as well as in argon. Figure 5.3.8 shows the results of this testing for Pd-13Cr and Pd-20Cr in Wt. percent. The resistance of the Pd-13Cr increased during the pre-oxidation soak in air as might be expected if an oxide coating were being formed. During the next 60 hours in argon followed by air, the resistance dropped, reaching a rate of approximately -18μΩ/Ω/hr at the conclusion of the testing in air. In contrast to Pd-13Cr, the resistances of the other binary alloys increased during the entire series of drift runs. The drift rate increased dramatically when the sample was exposed to air as shown in figure 5.3.8. The final drift rate of 290 μΩ/Ω/hr for Pd-20Cr in air was the highest of any binary alloy. Figures 5.3.9 and 5.3.10 show the drift of all four binary alloys over 30 hours in argon and in air. This series of tests indicates that a good protecive oxide layer is not formed at 1250 K for PdCr alloys containing more than 13 Wt. percent chromium.

The surface of a Pd-13Cr drop-cast sample was examined after 40 hours in air at 1250 K to determine the nature of the oxidized layer formed. The sample was plated with nickel and sectioned to reveal the oxide-metal interface. Figure 5.3.11 shows electron microprobe data in the spot mode for palladium and chromium along a line across the oxide-metal interface. The metal alloy is to the right and the surface film is to the left. The amount of chromium in the alloy appears to be uniformly distributed right up to the interface between the oxide film and the metal alloy substrate. The concentration of chromium in the surface film is more than three times greater than in the alloy. The fact that the chromium composition does not appear to be completely uniform across the surface layer is probably due to the size of the electron beam spot which necessarily controls the ultimate resolution of the system. The surface film also contains a small percentage of palladium which appears in the section to be near the surface of the film. A SEM image and oxygen density map of this sample are shown in figure 5.3.12. This examination reveals that the oxidized surfaces are irregular in thickness. Also of interest is the observation that the palladium seen in the surface film in the profile of figure 5.3.11 appears as distinct inclusions in the film and at its surface.

The observation of inclusions of Pd in the surface oxide films suggests that oxygen was the major diffusing species. These palladium inclusions probably do not contain any chromium. Once these inclusions or projections of palladium have lost their chromium, they may act as faster paths for the diffusion of oxygen than would the oxide scale. The thickness of the oxide scale varied in our measurements from 2 to 15 μm with examples of both palladium on the outside surface of the scale and extending into it, and oxide scale protrusions extending into the palladium alloy substrate. This non-uniform film thickness may indicate preferential oxidation at grain boundaries or other defects and spallation.

The reproducibilities of the resistance curves for the binary alloys were evaluated by cycling a sample of each alloy to 1250 K at 50 K/min for five consecutive cycles. The results of this series of tests for cycles two through five are shown in Tables 5.3.2 and 5.3.3 for Pd-13Cr and Pd-22Cr, respectively. The largest deviation for either alloy is in the region 750 to 900 K and is associated with the largest divergence between the heating and cooling curves. The slight break in the heating curve for Pd-22Cr seen in figure 5.3.3 also occurred at this temperature. The overall standard deviation for both alloys shows a high degree of reproducibility which was typical of all four alloys.

A facility for forming rapidly solidified foils was utilized to produce Pd-13Cr resistivity samples in the form of strips approximately .008 cm thick. The technique used to produce these "splat" samples was described in Section 4.1. Figure 5.3.13 shows the relative change in resistance of one of these samples between room temperature and 1250 K. The thermal coefficient of resistance, alpha, for this splat-cast sample was 169 $\mu\Omega/\Omega/K$, the same as the value obtained for the two drop-cast Pd-13Cr samples described in Table 5.3.1.

Measurements of the drift in resistance of this foil sample at 1250 K in air are presented in figure 5.3.14. The data shows a significant positive rate of drift which had not reached a stable condition even after 50 hours.

## 5.4 Mechanical and Other Properties of Cast Materials

Figure 5.4.1 shows the linear thermal expansion of Pd-13Cr versus temperature for both heating and cooling at 2 K/min. These measurements were made in argon in the differential mode with a similarly sized rod of pure platinum as the reference standard. Figure 5.4.2 presents computer generated curves which show how the coefficient of thermal expansion varies with temperature. A value of $14.6 \times 10^{-6}/K$ is a good average value for this coefficient over the range from room temperature to 1250 K.

Table 5.4.1 contains a summary of data compiled from stress-strain testing of Pd-13Cr at temperatures from R.T. to 1250 K. Stress and strain data from Table 5.4.1 are plotted vs. test temperature in figures 5.4.3 and 5.4.4. The deflectometer used for the tests above 1100 K is not as reliable as the extensometer since it is not in direct contact with the test sample within the gage section. Any elongation taking place outside the gage section during the test, such as slippage at the grip face or tightening of the load train, will result in an error in the strain reading. This probably accounts for some of the scatter in the strain data above 1100 K. Figure 5.4.5 shows stress-strain curves for this alloy at 1100 K and at 1250 K.

In order to measure the gage factor of Pd-13Cr at room temperatures, electrical leads were spot welded to a tensile sample to permit a four-wire measurement of resistance to be made during tensile testing. A computer was programmed to read and record the load, strain and resistance every 10 seconds during the test. Figure 5.4.6 shows a plot of the simultaneously recorded stress and resistance vs. strain for Pd-13Cr at room temperature. The data indicates that the gage factor changes after the sample yields. Figure 5.4.7 shows data for the same sample cycled at various strain rates below the yield stress. This plot shows that, within the range of conditions used, the gage factor is constant below the yield and is not strain rate dependent.

All of the Pd-13Cr rods used for resistivity, tensile, oxidation, and thermal expansion testing were cast from the same lots of the pure elements. The results obtained from a chemical analysis of one of these drop cast rods are presented in Table 5.4.2. The major impurity present is 0.1 weight percent platinum (1000 ppm). Because this is a similar noble metal which does not react with oxygen, its presence is probably not harmful. The next major impurity is iron at 200 ppm. The importance of such minor impurities is not known.

## 5.5 Fabrication of Sputtered Samples

Two different sized Hastelloy-X substrates were produced. The smaller 15 mm x 19 mm plates were sputtered with a stripe of Pd-13Cr which was 6 μm thick and 6.4 mm x 12 mm in area. The larger plates, which measured 19 mm x 80 mm, were coated with the sputtered Pd-13Cr resistance strain gage pattern shown previously in figure 4.1.2. This pattern consists of 10 lines (5 loops) which were only .13 mm wide compared with the lead films which were 6.4 mm wide. The total area of the grid sensor is 13 x 13 mm. A total of 16 sputtered Pd-13Cr sputtered samples of this design were prepared on Hast-X substrates. In addition, 5 sputtered samples of the smaller dimensions described above were also prepared on alumina substrates. Descriptions of all these samples and test results are presented in Tables 5.5.1 and 5.5.2.

No problems of adhesion were observed after sputtering with any of the above samples, regardless of substrate composition or surface finish. Scanning Electron Microscope examinations of the as-sputtred films showed that they all had a "corn cob" type structure and that there were nonuniformities in the sizes of the growth nodules. Figure 5.5.1 shows the surface structure of a typical sputtered film.

Because the as-sputtered films would not be in their thermodynamic lowest energy stae, the sputtered samples were heat treated to anneal and recrystallize the Pd-13Cr films prior to testing. Recrystallization would be expected to relieve the high internal stresses in the films and, most importantly, remove most of the high energy grain boundaries between nodules which would be pathways for enhanced grain boundary diffusion of oxygen and sources of cracking when the films were subjected to tensile strains. The original procedure for carrying out this recrystallization consisted of encapsulating the samples in quartz ampules under vacuum and heating to 1473 K for 2 hours. It was subsequently discovered that the films were being contaminated during this process by reactions with silica and that these reactions could not be prevented even by carefully wrapping the samples inside tantalum foils. Subsequent heat treatments were done in an impervious, clean alumina tube containing tantalum trays to getter any oxygen present and purged with gettered argon from a special inert gas purifier. The purifier lowered the oxygen content of the purging atmosphere from approximately 1-3 ppm oxygen from a bottled argon source to less than $1 \times 10^{-7}$ ppm $O_2$. It was also found that the sputtered Pd-13Cr films could be completely recrystallized at 1370 K if the time at temperature was increased from 2 hours to 12 hours. The structure of the recrystallized Pd-13Cr film is shown in Fig. 5.5.2.

The recrystallized films appeared to be flatter and the deep grooves which appeared to form between some of the as-sputtered nodules were no longer present. The films, however, contain some holes which generally extend all the way through the films to the alumina surface below. It is believed that these holes are formed as a result of the breakout of some of the larger growth nodules shown in figure 5.5.1.

Scanning electron microscope (SEM) examinations of samples recrystallized in very pure argon revealed the presence of balls of palladium on the surface of the sputtered alumina insulating layer adjacent to the PdCr films. These were determined to be Pd balls by energy dispersive analysis. These balls were not observed on samples recrystallized in air or using bottled argon. The presence of a very small concentration of oxygen was sufficient to prevent the formation of these balls.

The data to be presented in more detail in Section 5.6 revealed the need to develop protective overcoats to prevent excessive oxidation of the Cr in these sputtered films. To address this problem, three samples were overcoated with sputtered aluminum. The plan was to provide a sealing coat of alumina ($Al_2O_3$) by converting this metal coating to the oxide form by oxidation in place. Attempts to oxidize these overcoats were not successful because the initial aluminum oxide formed was so impervious to any further oxidation. Figure 5.5.3 shows "spurs" of alumina formed preferentially along the edges of the PdCr grid lines. Apparently the aluminum under the oxide melted, the volume expansion ruptured the thin oxide surface, and more oxidation occurred again. The process was repeated until all of the aluminum metal was oxidized or dissolved in the alloy.

Electron microprobe measurements were made of the composition of the sputtered film on sample HX-24 after it had been heated for 2 hours at 1370 K in flowing argon (1-2 ppm $O_2$). Because some oxidation of the surface of the film had occurred, these measurements were made on surfaces cleaned by grit blasting as well as on surfaces which had not been cleaned in this manner. The average composition at two different locations in the grit blasted areas was 79.4 Pd, 15.9 Cr and 4.7 Al, all in Wt. percent. The average compositions at two different locations in areas which were not grit blasted was 61.8 Pd, 35.1 Cr and 3.1 Al, all in Wt. percent. The higher concentration of Cr for the areas not cleaned by grit blasting is consistent with the formation of a surface protective film of chromium oxide.

The presence of aluminum was unexpected. Some of the aluminum present in the grit-blasted areas might have been due to residual particles of alumina grit embedded in the film. The presence of a small amount of aluminum might be beneficial in helping to form a good protective oxide film and in reducing the thermal coefficient of resistance. Alternatively, its presence might result in ordering effects at intermediate temperatures.

It was not possible to conduct an electron microprobe analysis of the target* because that would have required cutting away a piece of the target for examination. It was discovered, however, that the whole target could be put inside the scanning electron microscope so that an energy dispersive analysis could be made of an area in the center of the target (about 2 cm x 2 cm). Although this did not provide a quantitative analysis, peaks were observed for Al as well as small peaks for Si and Fe. Further examinations in the spot mode revealed areas rich in Al and Mo. More complete electron microprobe analyses of sputtered PdCr films will be made in later tasks in this program.

### 5.6 Electrical Properties of Sputtered Pd-13Cr

Three sputtered Pd-13Cr resistivity samples were tested during Task 2. Sample HX-8R was subjected to a heat treatment of 12 hrs in air at 1370 K to recrystallize the PdCr and to form a protective chromia ($Cr_2O_3$) layer. This heat treatment reduced the gage resistance from 140 Ω as-sputtered to 32 Ω. This sample was then cycled twice to 1250 K at 10 K/min in the thermal resistivity measuring apparatus before testing was discontinued because the power leads shorted through to the substrate. A plot of the data obtained is presented in Fig. 5.6.1. The value of alpha (the thermal coefficient of resistance) for this sample was 2000 μΩ/Ω/K compared to 168 μΩ/Ω/K for drop

*Materials Research Corp., Orangeburg, NY, composition 86 Pd, 14 Cr (Wt %)

cast Pd-13Cr. This result indicates that in very thin films, most of the chromium must be consumed by oxidation in order to form the protective oxide scale.

To lower the amount of Cr lost during the formation of an oxide layer, the heat treatment temperature for the next sample, (HX-9R), was lowered to 1250 K. At this temperature the sample did not recrystallize. This sample also experienced a large drop in gage resistance during heat treatment from 165 Ω to 56 Ω indicating a substantial loss of Cr.

This sample was then cycled four times to 1250 K, the first two cycles being at 10 K/min and the last two at 50 K/min. The results from the first cycle at 50 K/min are shown in figure 5.6.2. Leads from one tab of the PdCr film and one from the thermocouple spot-welded to the substrate were connected to an ohmmeter to permit measurements to be made of the resistance from the film to the substrate during various thermal exposures. For the cycle plotted in figure 5.6.2, the resistance was greater than 20 megohm at temperatures below 830 K. Above 830 K the resistance dropped steadily from 20 megohms at 830 K to a low of 2.6 megohms at 1100 K. Above 1100 K the resistance rose to 4.3 megohms at 1250 K.

The break in the resistivity curve at 1050 K on heating and 975 K on cooling occurred during all four cycles. The magnitude of this break was greater at the slower heating rate although the temperature at which it occurred did not vary. This break occurs in the temperature region where the resistance to the substrate is at its minimum. Some leakage to the substrate, which is grounded through the thermocouple, may account for the decrease in sample resistance above 1050 K. A similar break was also observed during testing of Hx-8R. The following values of alpha may be compared:

| | |
|---|---|
| HX-9R, RT to 1050 K | 1570 μΩ/Ω/K |
| HX-8R, RT to 1050 K | 2000 μΩ/Ω/K |
| Drop Cast Pd-13Cr | 168 μΩ/Ω/K |

Following these initial cycles, the sample was heated to 1250 K for a 50 hr drift check. The drift data for HX-9R compared with data for thicker film samples is shown in figure 5.6.3. The drift rate during the last 20 hours had stabilized at -227 μΩ/Ω/hr. Two cycles run at 50 K/min after the drift check showed that alpha had increased to 2560 μΩ/Ω/K (300-1050 K), indicating that the sample lost more chromium during the drift period. The second cycle at 50 K/min after the drift check was made with the sample thermocouple detached from the sample, leaving the substrate ungrounded. The resistivity curve still had a break at 1050 K, leading to the conclusion that this event was not simply due to a leakage to ground at high temperatures. Sample resistance at 300 K changed from 56 ohms at the start of testing to 45 ohms at the end of testing. This decrease in resistance was probably due to the loss of Cr from the alloy by oxidation which removed some of the scattering centers from the alloy.

# 6.0 DISCUSSION OF RESULTS

## 6.1 FeCrAl Type Alloys

The final form in which these materials will be used as the strain sensitive elements in a strain gage will probably be as a sputtered film (the preferred final fabrication approach for use on a gas turbine blade or vane) or in the form of a very fine wire, typically .0025 cm in diameter. Drop casting material in much larger volumes was selected as the primary method for sample fabrication in this program because of cost, the ability to easily examine microstructures, to more easily permit mechanical tests on the different alloys, and to generally facilitate the ease with which an iterative alloy development program could be pursued.

The fine polish given to heat treated samples prior to the oxidation studies was to ensure a uniform starting condition and that relatively clean metal surfaces would be exposed for oxidation attack. This procedure is relatively standard for use in this type of testing. Apparently all of the very thin coatings formed in the oxidation tests were protective in the sense that none of the samples continually lost weight. Instead of indicating excellent resistance to oxidation, a zero weight gain could result from a fortutious balance between weight gain due to reaction with oxygen and weight loss due to the loss of oxide scale by spallation.

The results obtained from the oxidation of the cast rods were probably too insensitive for our purposes. A 2 μm thick oxide film on these rod samples would result in an extremely small effect based on a weight-loss criterion. This same result, however, would be extremely significant if it occurred on a 6.5 μm thick sputtered film while electrical resistance mesurements were being made.

If the only problem with the FeCrAl alloy is simply oxidation, a successful solution might be to find a suitable protective overcoat to seal the surfaces from oxidation. Although efforts to develop this alloy have been discontinued, it would be useful to determine if this alloy even uncoated might not be useful to satisfy static strain measurement needs at other temperatures below 1250 K.

## 6.2 PdCr Type Alloys

If no metallurgical changes take place in an alloy as the temperature is changed, then the response of the electrical resistivity to changes in temperature should be linear. The increasing thermal agitation of the atoms as the material is heated and the consequent scattering of any electrons drifting throughout the lattice should cause the measured resistivity to increase in

direct proportion to the absolute temperature. In the case of Pd-13Cr (in Wt. percent), this linear behavior was seen in both the drop cast and splat cooled samples, figures 5.3.1 and 5.3.13, respectively.

These results indicate that Pd-13Cr is a very stable alloy in which the Cr is retained in solid solution over this full range of temperatures. Provided that there are no other effects to modify its resistance, such as the loss of some material by oxidation, this alloy would not be expected to show any appreciable drift in electrical resistance with time. More obvious non-linear breaks in similar curves for alloys containing higher concentrations of Cr indicate that ordering or clustering reactions are occurring and that these alloys have a greater potential to have electrical drift problems at some intermediate temperatures.

Although the metallurgical stability of the Pd-Cr alloy appears to be satisfactory, its thermal coefficient of resistance is too high to meet our coefficient goals and some form of thermal compensation will have to be developed and demonstrated in a later task of this program.

The lower curve of figure 5.4.6 suggests that the gage factor of the Pd-13Cr alloy is erratic and varies with strain. This is probably an incorrect conclusion, the data more likely is reflecting the fact that this sample is not straining uniformly. Prior to testing, this sample had been annealed for 2 hr. at 1470 K which produced large grains in the material. The typical grain size was of the order .03 cm. Because the strain gages were of similar size, .03 x .05 cm, the data is probably reflecting the different behaviors of several different grains which have different crystallographic orientations to the axis of loading. The gage factors of sputtered Pd-13Cr films will be more fully examined in Task 8 of this program.

The stress-strain curves shown in figure 5.4.5 suggest that the elastic modulus of the Pd-13Cr alloy, the slope of the initial elastic portion of these curves, has been significantly reduced by increasing the temperature from 1100 K to 1250 K. This is probably incorrect. Because the strain measurements at 1250 K were deduced from deflectometer measurements of cross-head motion, the measurements at 1250 K include the compliance of other loading components in addition to that of the sample. On this scale, the elastic slope of the 1250 K data should be almost indistinguishable from that at 1100 K. Given the yield stress at 1250 K shown in figure 5.4.5, the elastic limit at 1250 K must be well under 2000 microstrain. We believe that it would be preferable for our application if the strain gage alloy was not required to flow plastically during use.

Several additional factors may have some bearing upon this conclusion as applied to sputtered Pd-13Cr strain gages. In the first place, as mentioned above, this material used for the mechanical testing experiments had an extremely large grain size. In contrast, even when the sputtered foils have been recrystallized, their grain size is normally restricted by the foil dimensions to be no larger that the thickness of the foil, approximately 6 μm. This smaller grain size should cause the yield strength of the foil and the yield stress to be appreciably higher. In addition, the foil is intimately bonded to an aluminum oxide layer and this should further act to limit the initiation and extent of plastic flow in a sputtered foil. If it were necessary or desirable to also encase the top surface of the sputtered foil with a nonductile ceramic, this would probably also further reduce the ease with which plastic flow could be initiated in the alloy. The actual effect of these factors on the properties of the sputtered foil will be determined in a subsequent task of the program.

## 7.0 SUMMARY AND CONCLUSIONS

Results are presented for the first two tasks in a contract to develop resistive strain gage systems for use up to 1250 K on blades and vanes in gas turbine engines under test. The objective of these two tasks was to further improve and evaluate two static strain gage alloys identified as candidates in a previous program. Improved compositions were not found for either alloy. Further efforts on the Fe-11.9Al-10.6Cr weight percent alloy were discontinued because of time dependent drift problems at 1250 K in air. When produced as a 6.5 micrometer thick sputtered film, the Pd-13Cr weight percent alloy is not sufficiently stable for this use in air at 1250 K and a protective overcoat system will need to be developed.

The major conclusions and accomplishments from this work are listed below:

1. Weight loss experiments to measure the effects of minor additions of Hf, Zr, Sc, and Y on the oxidation reistance at 1250 K of an alloy of nominal composition Fe-10.6Cr-11.9Al in weight percent did not result in the identification of any improved alloy candidates.

2. Major changes in the shapes of the resistance versus temperature curves of the Fe-10.6Cr-11.9Cr alloy can result from changes in composition of as little as 1 to 2 percent.

3. Thermal soaking of the Fe-10.6Cr-11.9Al alloy in air at 1250 K resulted in changes in the resistivity versus temperature curves. The total change in resistance from RT to 1250 K increased from 1.5 percent to 3.3 percent after soaking for a total of 105 hrs at 1250 K. Further work on this alloy was discontinued as a result of these observations.

4. Samples of both types of alloys were prepared by arc melting on a cold hearth and then drop casting into fused silica tubes. Additional samples of the Pd-13Cr alloy were also evaluated after preparation by splat cooling and by sputtering.

5. Metallographic examinations and estimates were made of the solubilities of Er, Hf, Gd, La, Ni, Re, Ta, Co, Y, Mo and W in an alloy with the nominal composition of Pd-13Cr, in weight percent.

6. The Pd-13Cr alloy forms an adherent, self-protective scale of $Cr_2O_3$ which effectively prevents further oxidation of the Cr in solid solution at 1250 K in air when the alloy is prepared as a 460 micrometer thick foil by drop casting and grinding. The protection from

this scale is thickness dependent and, when the alloy is prepared as a 6.5 micrometer thick sputtered film, the amount of oxidation attack was too extensive to meet the goals of this program.

7. Sputtered films of the Pd-13Cr alloy can be completely recrystallized by heating to 1370 K for at least 2 hr. in a very pure argon atmosphere. This treatment should increase its fracture strain and its resistance to internal oxidation.

8. A sealed overcoat system must be developed in subsequent tasks of this contract in order to permit a sputtered thin film of Pd-13Cr to successfully meet the program goals.

9. The average thermal expansion of Pd-13Cr from room temperature to 1250 K is $14.6 \times 10^{-6}$/K which is a good match with nickel-base superalloys.

10. The 0.02 percent yield strength of drop cast and annealed Pd-13Cr decreases from $1.10 \times 10^{3}$ MPa at room temperature to $12 \times 10^{3}$ MPa at 1250 K. The elastic limit at 1250 K is approximately 500 microstrain. This limit may be appreciably greater when the alloy is prepared as a sputtered film on a sputtered alumina insulation layer.

11. The room temperature gage factor of the Pd-13Cr alloy is about 1.8 within the elastic range which extends to approximately 5000 microstrain.

12. Because of the high thermal coefficient of resistance of Pd-13Cr, a thermal compensation system will need to be developed in subsequent tasks of the program.

## 8.0 REFERENCES


1. Stetson, C: Demonstration Tests of Burner Liner Strain Measuring System, NASA CR-174743.

2. Hulse, C. O., Bailey, R. S., and Lemkey, F. D.: High Temperature Static Strain Gage Alloy Development Program, NASA CR-174833.

3. Hulse, C. O., Bailey, R. S., and Grant, H. P.: The Development of a High Temperature Static Strain Gage System. Turbine Engine Hot Section Technology 1985, NASA CP-2405, pp. 45-59.

4. Hulse, C. O., Bailey, R. S., and Grant, H. P.: High Temperature Static Strain Gage Program. Turbine Engine Hot Section Technology 1984, NASA CP-2339, pp. 71-76.

5. Whittle, D. P., and Stringer, J.: Philos. Trans. R. Soc. London, Ser., 1980, Vol. A295, pp. 309-29.

6. Smeggil, J. G., Funkenbush, A. W., and Bornstein, N. S.: A Relationship Between Indigenous Impurity Elements and Protective Oxide Scale Adherence Characteristics, Metall. Trans. A, Vol. 17A, 1986, pp. 923-31.

7. Tien, J. K., and Pettit, F. S.: Metall. Trans., 1972, Vol. 3, pp. 1587-99.

8. Grant, H. P., Prcybyszewski, J., and Claing, R. J.: Turbine Blade Temperature Measurements Using Thin Film Temperature Sensors, NASA CR-165201.

**TABLE 5.1.1 - OXIDATION RESULTS FOR FeCrAl ALLOYS**

| Rank | Composition | Alloy | Weight Gain ($mg/cm^2$) | | | |
|---|---|---|---|---|---|---|
| | | | 2 Hrs | 12 Hrs | 26 Hrs | 50 Hrs |
| 1 | Fe-11.9Al-10.6Cr | 1 | .08 | .05 | .06 | .07 |
| 2 | Fe-11.9Al-10.6Cr-0.5Co | 7 | .05 | .00 | .06 | .12 |
| 3 | Fe-24Al-7Cr | 5 | .10 | .09 | .14 | .14 |
| 4 | Fe-11.9Al-10.6Cr-0.2Se | 13 | .07 | .07 | .12 | .19 |
| 5 | Fe-11.9Al-10.6Cr-0.1Y | 6 | .03 | .10 | .17 | .19 |
| 6 | Fe-11.9Al-10.6Cr-0.05Sc | 12 | .06 | .06 | .14 | .20 |
| 7 | Fe-11.9Al-10.6Cr preoxidized | 2 | .01 | .06 | .10 | .21 |
| 8 | Fe-11.9Al-10.6Cr-0.1Zr | 8 | .05 | .13 | .17 | .22 |
| 9 | Fe-11.9Al-10.5Cr-0.25Hf | 11 | .08 | .14 | .17 | .25 |
| 10 | Fe-11.9Al-10.6Cr-0.25Zr | 9 | .17 | .22 | .31 | .36 |
| 11 | Fe-11.9Al-10.6Cr-0.1Y-0.25Hf | 10 | .14 | .24 | .33 | .41 |
| 12 | Fe-38Ni-20Cr-4Al | 3 | .03 | .21 | .38 | .51 |
| | Fe-20Cr-17Al | 4 | Lost during testing - No data | | | |

**TABLE 5.1.2 - RESULTS OF PdCr TYPE ALLOY SOLUBILITY STUDY**

(After Repeated Arc-Meltings)

| Samples | Composition (wt%) | Comments** |
|---|---|---|
| PdCr-1 | Pd-16Cr-7Gd | Second phase, approx. 8 v/o |
| PdCr-2 | Pd-16Cr-10Gd | Second phase, approx. 8 v/o |
| PdCr-3 | Pd-16Cr-7Er | Second phase, approx. 10 v/o |
| PdCr-4 | Pd-16Cr-10Er | Second phase, approx. 10 v/o |
| PdCr-5 | Pd-16Cr-8La | Second phase, approx. 40 v/o |
| PdCr-6 | Pd-16Cr-11La | Second phase, approx. 40 v/o |
| PdCr-7 | Pd-16Cr-5Ni | Apparently single phase (1000X) |
| PdCr-8 | Pd-16Cr-8Ni | Apparently single phase (1000X) |
| PdCr-9 | Pd-16Cr-5Re | Second phase, approx. 5 v/o |
| PdCr-10 | Pd-16Cr-3Ta | Apparently single phase (1000X) |
| PdCr-11 | Pd-16Cr-6Y | Second phase, approx. 5 v/o |
| PdCr-12 | Pd-13Cr | Apparently single phase (1000X) |
| PdCr-13 | Pd-18Cr | Apparently single phase (1000X) |
| PdCr-14 | Pd-22Cr | Apparently single phase (1000X) |
| PdCr-15 | Pd-16Cr-6Ta | Apparently single phase (1000X) |
| PdCr-16 | Pd-16Cr-10Ni | Apparently single phase (1000X) |
| PdCr-17 | Pd-16Cr-8Co | Apparently single phase (1000X) |
| PdCr-18 | Pd-7Cr-3Gd | Two phase, eutectic |
| PdCr-19 | Pd-7Cr-3Er | Small eutectic present, approx. 1.5 v/o |
| PdCr-20 | Pd-7Cr-3La | Two phase |
| PdCr-21 | Pd-16Cr-5Mo | Apparently single phase and over etched |
| PdCr-22 | Pd-16Cr-10Mo | Apparently single phase and over etched |
| PdCr-23 | Pd-16Cr-6Mo-3Ta | Apparently single phase and over etched |
| PdCr-24 | Pd-16Cr-6Mo-3Ni | Apparently single phase and over etched |
| PdCr-25 | Pd-18Cr-6Mo | Apparently single phase and over etched |
| PdCr-26 | Pd-16Cr-5W | Apparently single phase and over etched |
| PdCr-27 | Pd-16Cr-10W | Apparently single phase and over etched |
| PdCr-28 | Pd-16Cr-6W-3Ta | Apparently single phase and over etched |
| PdCr-29 | Pd-16Cr-6W-3Ni | Apparently single phase and over etched |
| PdCr-30 | Pd-18Cr-6W | Apparently single phase and over etched |
| PdCr-31 | Pd-16Cr-7Ta | Probably single phase |
| PdCr-32 | Pd-16Cr-12Ta | May be single phase |
| PdCr-33 | Pd-18Cr-12Ta | Looks single phase but with "holes" |
| PdCr-34 | Pd-16Cr-4Re | Second phase, approx. 5 v/o |
| PdCr-35 | Pd-20Cr | Apparently single phase |

*Standard Heat Treatment = 2 hrs at 1470 K, cool in 1 hr to 1270 K, cool to 770 K at approx. 25 K/hr in argon; samples held in individual alumina tubes wrapped in molybdenum foil

**Etchant - (15) HCL + (75) Methanol, 10V-DC for 30 sec, rinse in alcohol

**TABLE 5.1.3 - OXIDATION OF CAST PdCr TYPE ALLOYS**

(50 hrs in Static Air at 1250 K)*

| Sample # | Alloy Composition (wt%) | Total Wt. Gain, ΔW/Area (mg/cm²) .25 hr | 1 hr | 4 hr | 12 hr | 26 hr | 50 hr |
|---|---|---|---|---|---|---|---|
| PdCr-8-Ox | Pd-16CR-8Ni | .10 | .06 | .14 | .13 | .33 | .38 |
| PdCr-10-Ox | Pd-16Cr-3Ta | .15 | .12 | .18 | .24 | .46 | .53 |
| PdCr-12-Ox | Pd-13Cr | .11 | .08 | .14 | .23 | .31 | .34 |
| PdCr-13-Ox | Pd-18Cr | .12 | .09 | .17 | .24 | .39 | .47 |
| PdCr-15-Ox | Pd-16Cr-6Ta | .19 | .18 | .24 | .35 | .56 | .60 |
| PdCr-35-Ox | Pd-20Cr | .11 | .10 | .15 | .21 | .39 | .46 |
| PdCr-36-Ox | Pd-16Cr-6Mo | .22 | .20 | .29 | .41 | .68 | .88 |

*Pretest heat treatment - 2 hrs in argon at 1470 K, samples held in individual alumina tubes, wrapped in tantalum foils

TABLE 5-2 - SUMMARY OF DATA FOR CAST FeCrAl TYPE ALLOYS

| Sample Number | Alloy Composition (wt %) | Heat Treatment (argon) | Temp. Coefficient of Resistance: Before 1250K Drift 50K/min (μΩ/Ω/K) | Temp. Coefficient of Resistance: After 1250K Drift 50K/min (μΩ/Ω/K) | Temp. Coefficient of Resistance: After 1250K Drift 250K/min (μΩ/Ω/K) | ΔR/RVs Temp. | Total Drift (μΩ/Ω in 10 hrs): 1250K | Total Drift (μΩ/Ω in 10 hrs): 1100K | Remarks |
|---|---|---|---|---|---|---|---|---|---|
| K-mod-3-1 | Fe-11.0Cr, 10.3A1* | None | -27.4 | N/D | N/D | | N/D | N/D | |
| K-mod3-2 | Fe-9.9Cr, 11.2A1* | None | -27.6 | N/D | N/D | | N/D | N/D | |
| A83-317-2 | Fe-12.2Cr, 8.95A1** | None | +9.26 | +16.8 | N/D | | -947 | N/D | |
| A83-317-1 | Fe-12.2Cr, 8.95A1** | 1473K/2 hrs | +15.3 | +24.4 | +25.5 | | +1,464 | -80 | After 1100K drift, TCR @ 50K/min=25.7 |
| A83-317-1 | Fe-12.2Cr, 8.95A1** | 1250K/65 hrs | +30.1 | +35.0 | N/D | | +1,295 | N/D | |
| A83-415-1 | Fe-12.8Cr, 9.33A1** | None | -3.05 | +1.53 | N/D | Nonlinear 600→825K | +1,814 | N/D | |
| A83-415-2 | Fe-12.8Cr, 9.33A** | 1473K/2 hrs + 1250K/75 hrs | -1.26 | +1.13 | +1.12 | Nonlinear 600→825 | +4,123/ 5 hrs | | |
| A83-415-3 | Fe-12.8Cr, 9.33A1** | None | +6.5 | +7.7 | N/D | | 1,229 | N/D | Preoxidized; 10 hrs at 1250 K |
| A83-416-1 | Fe-11.7Cr, 10.3A1** | None | -36.9 | -24.3 | N/D | Nonlinear 600→825K | +4,471 | N/D | N/D |
| A83-416-2 | Fe-11.7Cr, 10.3A1** | 1473K/2 hrs + 1250K/75 hrs | -38.2 | -30.0 | N/D | Nonlinear 600→825 | +3771 | N/D | |
| A83-421-1 | Fe-11.4Cr, 9.54A1** | | N/D | | | | | | |
| A83-421-2 | | | N/D | | | | | | |
| Fe-3-1 | Fe-38Ni, 20Cr, 4A1 | None | +289 | +320 | +371 | Linear | -6,034 | N/D | |
| Fe-14 | Fe-13Cr, 22A1 | 1573K/2 hrs | -54.0 | N/D | -56.5 | Smooth | N/D | N/D | |
| K-5 | Fe-12.3Cr, 9.4A1* | 1473K/3 hrs | -6.38 | N/D | N/D | | (~0/3 hrs) -1824/3 hrs | N/D | 6/2/82 |
| K-5 | | Cycled | -4.2 | | | | | | 8/29/83 |
| K-5 | | Cycled | +1.8 | | | | | | 9/13/83 |
| K-5 | | Cycled | | | | | -1,250 | -70 | 10/14/83 |
| K-5 | | +10 hrs 1250K | - | +17.9 | | | | | 10/17/83 |

*From Electron Microprobe
**From Chemical Analyses

**TABLE 5.3.1 - SUMMARY DATA FOR CAST PdCr TYPE ALLOYS**

| Sample Number | Alloy Composition (wt %) | Heat Treatment (argon) | Temp. Coefficient of Resistance Before 1250K Drift 50K/min (μΩ/Ω/K) | Temp. Coefficient of Resistance After 1250K Drift 50K/min (μΩ/Ω/K) | Temp. Coefficient of Resistance After 1250K Drift 250K/min (μΩ/Ω/K) | ΔR/RVs Temp. | Total Drift (μΩ/Ω in 10 hrs) 1250K | Total Drift (μΩ/Ω in 10 hrs) 1100K | Remarks |
|---|---|---|---|---|---|---|---|---|---|
| PdCr-12-1 | Pd13Cr | 1470K/2 hrs | 168.4 | 160.6 | 159.0 | Linear | -683 | +298 | |
| PdCr-12-2 | Pd13Cr | 1470K/2 hrs | 169.9 | 170.5 | 166.2 | Linear | -154 | N/D | |
| PdCr-13-1 | Pd18Cr | 1470K/2 hrs | 136.5 | 137.6 | 136.9 | Linear | ~+1,000 | -200 | |
| PdCr-13-2 | Pd18Cr | 1470K/2 hrs | 142.5 | 140.3 | 138.3 | Linear | +504 | N/D | |
| PdCr-35-1 | Pd-20Cr | 1470K/2 hrs | 132.6 | 132.8 | N/D | Slight Break @ 825 K | +2,400 | N/D | |
| PdCr-14-1 | Pd22Cr | 1470K/2 hrs | 119.2 | 119.7 | 120.1 | Break @ 825K | +3,898 | +200 | Good |
| PdCr-14-2 | Pd22Cr | 1470K/2 hrs | 126.9 | 126.0 | 124.7 | Linear | +422/+113 | | PreOx 1250K/10 hrs |
| PdCr-10-1 | Pd16Cr3Ta | 1470K/2 hrs | 128.0 | 131.6 | 135.7 | Break @ 950K | +1,047 | +632 | |
| PdCr-15-1 | Pd16Cr6Ta | 1470K/2 hrs | 169.1 | 165.1 | 149.1 | Break @ 375&1050K | +5,357 | +1,190 | Steeper slope 300-375 |
| PdCr-8-1 | Pd16Cr8Ni | 1470K/2 hrs | 155.6* | 157.4 | 157.0 | Slight Break @ 750K | - | - | Drift data suspect *250K/min |
| PdCR-16-1 | Pd16Cr10Ni | 1470K/2 hrs | 157.1 | 158.1 | 157.8 | Slight Break @ 750K | +450 | -130 | Good |
| PdCr-36-1 | Pd16Cr6Mo | 1470K/2 hrs | 129.2 | 119.6 | N/D | Break @ 825K | +3,559 | +200 | Good |
| PdCr-36-2 | Pd16Cr6Mo | 1470K/24 hrs | 201.3 | 167.5 | N/D | | +2,450 @ 2 hrs -1,400 @ 10 hrs | N/D | PreOx 1250K/10 hrs |
| PdCr-17-1 | Pd16Cr8Co | 1470K/2 hrs | 169.4 | 169.7 | 170.4 | Linear | +800 | -100 | |
| PdCr-37-1 | Pd5Cr2Er | 1470K/2 hrs | 395.1 | 452.4 | N/D | Linear | | N/D | |

**TABLE 5.3.2 - HEATING AND COOLING REPRODUCIBILITY OF Pd-13Cr (Wt %)**

**(Sample PdCr-12-2, 50K/min)**

| Temp. (K) | Avg. ΔR/R (Heat&Cool) | Std. Dev. (ΔR/R) | Difference in apparent strain in microstrain from avg. (G.F. = 2.0) | | | | | | | |
|---|---|---|---|---|---|---|---|---|---|---|
| | | | Cycle #2 | | Cycle #3 | | Cycle #4 | | Cycle #5 | |
| | | | Heat | Cool | Heat | Cool | Heat | Cool | Heat | Cool |
| 300 | .000019 | .000035 | -9 | 22 | -9 | 8 | -9 | -20 | -9 | 29 |
| 375 | .012708 | .000225 | 102 | -92 | 96 | -146 | 98 | -126 | 108 | -29 |
| 450 | .024873 | .000167 | 66 | -86 | 67 | -97 | 51 | -92 | 108 | -18 |
| 525 | .037336 | .000129 | 83 | -41 | 45 | -75 | 20 | -73 | 77 | -35 |
| 600 | .050246 | .000134 | 74 | -49 | 54 | -76 | 33 | -80 | 78 | -35 |
| 650 | .059032 | .000149 | 79 | -66 | 66 | -88 | 42 | -58 | 85 | -60 |
| 675 | .063434 | .000173 | 102 | -76 | 65 | -94 | 54 | -91 | 95 | -54 |
| 700 | .067867 | .000194 | 107 | -69 | 87 | -104 | 58 | -118 | 101 | -62 |
| 725 | .072294 | .000243 | 137 | -110 | 103 | -131 | 96 | -106 | 117 | -105 |
| 750 | .076717 | .000310 | 152 | -149 | 146 | -154 | 123 | -143 | 158 | -133 |
| 825 | .089293 | .000117 | 60 | -58 | 37 | -62 | 47 | -54 | 71 | -40 |
| 900 | .101574 | .000104 | 51 | -42 | 42 | -62 | 12 | -51 | 74 | -25 |
| 975 | .113633 | .000071 | 46 | -26 | 30 | -25 | -4 | -42 | 45 | -24 |
| 1050 | .125677 | .000061 | 40 | -29 | 37 | -18 | -10 | -34 | 30 | -16 |
| 1125 | .137862 | .000061 | 35 | -18 | 20 | -26 | 37 | -48 | 11 | -10 |
| 1200 | .150142 | .000065 | 41 | -28 | 40 | -23 | 0 | -41 | 30 | -19 |
| 1225 | .154231 | .000063 | 27 | -17 | 29 | -16 | 19 | -53 | 33 | -21 |
| 1250 | .158431 | .000043 | 30 | | -16 | | -15 | | 1 | |

Avg. Std. Dev. = .000130
Runs rezeroed between cycles

**TABLE 5.3.3 - HEATING AND COOLING REPRODUCIBILITY OF Pd-22Cr (Wt %)**

**(Sample PdCr-14-2, 50K/min)**

| Temp. (K) | Avg. ΔR/R (Heat&Cool) | Std. Dev. (ΔR/R) | Difference in apparent strain in microstrain from avg. (G.F. = 2.0) | | | | | | | |
|---|---|---|---|---|---|---|---|---|---|---|
| | | | Cycle #2 | | Cycle #3 | | Cycle #4 | | Cycle #5 | |
| | | | Heat | Cool | Heat | Cool | Heat | Cool | Heat | Cool |
| 300 | .000069 | .000078 | -34 | 22 | -34 | 19 | -34 | 36 | -34 | 62 |
| 375 | .009796 | .000035 | -21 | -4 | -4 | -24 | 8 | 0 | 19 | 27 |
| 450 | .018649 | .000061 | 5 | -48 | 20 | -40 | 27 | -8 | 35 | 9 |
| 525 | .027376 | .000065 | 6 | -43 | -0 | -40 | 27 | -20 | 42 | 29 |
| 600 | .036051 | .000062 | -30 | -24 | -31 | -18 | 8 | 11 | 32 | 52 |
| 650 | .041975 | .000065 | -30 | -8 | -44 | -10 | -7 | 26 | 13 | 60 |
| 675 | .045020 | .000054 | 12 | -17 | -35 | -21 | -9 | 8 | 12 | 52 |
| 700 | .048089 | .000056 | -33 | -13 | -21 | -20 | 9 | 15 | 11 | 54 |
| 725 | .051194 | .000035 | -10 | -18 | -5 | -18 | -6 | 9 | 14 | 33 |
| 750 | .054344 | .000053 | -1 | -37 | -10 | -30 | 18 | -3 | 43 | 20 |
| 825 | .063652 | .000186 | -94 | 76 | -106 | 71 | -70 | 83 | -73 | 113 |
| 900 | .073599 | .000068 | -27 | 16 | -50 | 13 | -17 | 47 | -22 | 39 |
| 975 | .083423 | .000034 | -13 | 0 | -4 | 9 | -13 | 37 | -13 | -3 |
| 1050 | .093139 | .000032 | -13 | -10 | -2 | -19 | 25 | 10 | 19 | -9 |
| 1125 | .102987 | .000034 | -6 | 9 | -11 | -9 | -1 | 29 | 14 | -25 |
| 1200 | .112722 | .000039 | 19 | 30 | -9 | 5 | -15 | 11 | -22 | -21 |
| 1225 | .116051 | .000054 | 37 | 32 | -43 | -7 | -16 | 17 | -13 | -7 |
| 1250 | .119287 | .000016 | 11 | | -2 | | -2 | | -7 | |

Avg. Std. Dev. = .000057

Runs rezeroed between cycles

**TABLE 5.4.1 - MECHANICAL PROPERTIES OF Pd-13Cr (Wt %) IN TENSION**

| Sample Number | Strain Meas. Method* | Heat Treatment (argon) | Test Temp. (K) | 0.2% Yield Strength (MPa) | Ultimate Tensile Strength (MPa) | Elastic Modulus (MPa x $10^3$) | Strain at Fracture % |
|---|---|---|---|---|---|---|---|
| PdCr-12-T1 | ε-gage | none | RT | 105 | 362 | 119 | 41.6 |
| PdCr-12-T2 | ε-gage | 1473K/2 hrs | RT | 123 | 384 | 124 | 26.9 |
| Average RT | - | - | RT | 114 | 373 | 121 | 34.2 |
| PdCr-12-T4 | Ext. | none | 700 | 106 | 278 | 100 | 18.0* |
| PdCr-12-T7 | Ext. | 1473K/2 hrs | 700 | 148 | 310 | 76 | 20.1 |
| PdCr-12-T5 | Ext. | 1473K/2 hrs | 1000 | 79 | 127 | 86 | 9.0 |
| PdCr-12-T10 | Ext. | 1473K/2 hrs | 1100 | 33 | >57 | 21 | >6.9 |
| PdCr-12-T11 | Ext. | 1473K/2 hrs | 1100 | 21 | 36 | 27 | 11.7 |
| PdCr-12-T8 | Deflect. | 1473K/2 hrs | 1150 | 26 | 43 | - | 26.3 |
| PdCr-12-T6 | Deflect. | 1473K/2 hrs | 1250 | ~ 0 | 3.6 | - | 14.3 |
| PdCr-12-T9 | Deflect. | 1473K/2 hrs | 1250 | 8.5 | 18 | - | - |

*Ext. = Clamp-on Extensometer
Deflect. = Deflectometer, Total Strain Between Crossheads

**TABLE 5.4.2 - CHEMICAL ANALYSIS OF ARC-MELTED Pd-13Cr (Wt %)**

**(Drop-Cast in Quartz Tube)**

| Element | Weight (%) |
|---|---|
| Palladium | 88.6 |
| Chromium | 13.3 |
| Carbon | 0.005 |
| Iron | 0.020 |
| Silicon | 0.005 |
| Nickel | 0.005 |
| Vanadium | 0.002 |
| Copper | 0.002 |
| Platinum | 0.100 |
| Gold | 0.002 |
| Rhodium | <0.001 |
| Niobium | <0.001 |
| Tungsten | <0.010 |

Table 5.5.1

Sputtered Pd-Cr, Fabrication, Parameters and Results

| Sputt Run No. | Sample Numbers* Small Plates $Al_2O_3$ | Small Plates Hast-X | Large Plates Hast-X | Sputtering Parameters** Volts | Time (Hrs) | Distance (cm) | Thickness (μm) | Rate (μm/Hr) | Resistance (ohms) As-sputtered To Ground (ohms) | As-sputtered Sample (ohms) | Sample After H. Treat. (% change) | Heat Treatments 1 Gas | 1 T(K) | 1 Hrs | 2 Gas | 2 T(K) | 2 Hrs | α after (ohms-ppm/K) |
|---|---|---|---|---|---|---|---|---|---|---|---|---|---|---|---|---|---|---|
| 1 | V | | | 900 | 16 | 6 | 6 | .38 | N.A | | | | | | | | | |
| | | 21S | | 900 | 16 | 6 | 6 | .38 | 3 | | | | | | | | | |
| | | 26R | | 900 | 16 | 6 | 6 | .38 | $>20 \times 10^{+6}$ | .6 | -50 | Ar | 1473 | 2 | Air | 1250 | 50 | |
| 2 | W | | | 1100 | 11 | 6 | 5 | .45 | N.A | | | | | | | | | |
| | | 24S | | 1100 | 11 | 6 | 5 | .45 | $>20 \times 10^{+6}$ | .56 | -8 | Ar | 1373 | 1.5 | | | | |
| | | 27R | | 1100 | 11 | 6 | 5 | .45 | $>20 \times 10^{+6}$ | | | | | | | | | |
| | | 23S | | 1100 | 11 | 9 | 2.8 | .25 | $>20 \times 10^{+6}$ | | | | | | | | | |
| 3 | X | | | 900 | 18.5 | 6 | 6.5 | .35 | N.A | | | | | | | | | |
| | | 25S | | 900 | 18.5 | 6 | 6.5 | .35 | $>20 \times 10^{+6}$ | | | Ar | 1373 | 13 | | | | |
| | | 28R | | 900 | 18.5 | 6 | 6.5 | .35 | $>20 \times 10^{+6}$ | | | | | | | | | |
| | | | HX1S | 900 | 18.5 | 6 | 6.5 | .35 | $>20 \times 10^{+6}$ | 119 | | Lost in Heat Treatment | | | | | | |
| | | | HX6R | 900 | 18.5 | 6 | 6.5 | .35 | $>20 \times 10^{+6}$ | 106 | | Lost in Heat Treatment | | | | | | |
| 4 | | 29R | | 900 | 18 | 6 | 6 | .34 | $>20 \times 10^{+6}$ | | Est. -79 | Air | 1373 | 12 | | | | |
| | | | HX2S | 900 | 18 | 6 | 6 | .34 | $>20 \times 10^{+6}$ | *** | | | | | | | | |
| | | | HX3S | 900 | 18 | 6 | 6 | .34 | $>20 \times 10^{+6}$ | 143 | | | | | | | | |
| | | | HX8R | 900 | 18 | 6 | 6 | .34 | $>20 \times 10^{+6}$ | 140 | -77 | Air | 1373 | 10 | | | | 2,000 |
| | | | HX9R | 900 | 18 | 6 | 6 | .34 | $>20 \times 10^{+6}$ | 165 | -66 | Air | 1250 | 10 | | | | 1,220 |
| 5 | Y | | | 900 | 18 | 6 | 6.5 | .36 | N.A. | | | | | | | | | |
| | Z | | | 900 | 18 | 6 | 6.5 | .36 | N.A. | | | Ar | 1373 | 13 | | | | |
| | | | HX5S | 900 | 18 | 6 | 6.5 | .36 | 20 x 10 | 122 | | Lost in Heat Treatment | | | | | | |
| | | | HX10R | 900 | 18 | 6 | 6.5 | .34 | 20 x 10 | 144 | -23 | Ar | 1373 | 5 | | | | 1,010 |

*Sample numbers, S=smooth, R=rough; small plates, 1.5 x 19 x .25mm ($Al_2O_3$) or 15 x 19 x 1.85mm (Hast-X), large plates 19 x 81 x 1.85 mm.

**Nominal Composition of Target, Pd-14Cr (Wt %).

*** Part of photoresist mask detached from surface after 17.4 hrs of sputtering causing opening in gage grid, right lead to ground resistance still $> 20 \times 10^{+6}$ ohms.

(1) Sputtering gas was argon at $5 \times 10^{-3}$ torr (.66 Pa).

(2) Parameters not evaluated are sputter etching, reactive sputtering, overcoats, gas pressure, gas composition and grounding of work piece.

(3) By the end of each sputtering run, considerable damage to photoresist had occurred, except in the case of sample 23/S, run at the larger sputtering distance.

(4) The as-sputtered adherence of all samples was excellent. Adherence at elevated temperatures was also excellent.

Table 5.5.2

Summary of Heat Treatment and Results for Sputtered PdCr

| Spec. | Type | As-Sputtered Resistance (Ω) | As-Sputtered Thickness (μm) | 1st Heat Treatment Temp. (K) | 1st Heat Treatment Atmosphere | Sputtered Overcoat | 2nd Heat Treatment Temp. (K) | 2nd Heat Treatment Atmosphere | Post-heat Treatment Resistance | Oxide-formed | Test Results and Comments |
|---|---|---|---|---|---|---|---|---|---|---|---|
| HX-21 | Test Patch | | 6 μm | | | No | | | | | 1/2 coated w/Au for SEM. Not used because of potent contamination. (might remove Au and reuse). |
| HX-26 | Test Patch | .3Ω | 6 μm | 1470K 2 hrs. | Vacuum (SIO ) Encapsulated | No | 1250K 50 hrs. | air | | | PdCr continuous, not grounded to substrate after oxidation. Recrystallized |
| HX-1 | Resistivity | 119Ω | 6.5 μm | 1470K 2 hrs. | Vacuum (SiO ) Encapsulated | No | | | | | Tab area peeled off substrate due to carbon (from SEM Grid melted). |
| HX-28 | Test Patch | | 6.5 μm | 1470K 2 hrs. | Vacuum (SiO ) Encapsulated | No | | | | | Rough surface. Recrystallized islands surrounded by areas which reacted or evaporated. |
| HX-25 | Test Patch | | 6.5 μm | 1370K 12 hrs. | Hi-Purity Argon | No | | | | | Post-heat treatment. SEM pictures taken. |
| HX-6 | Resistivity | 106Ω | 6.5 μm | 1370K 12 hrs. | Hi-Purity Argon | No | | | | | Sample recrystallized. Grid melted. Balls on $Al_2O_3$ near PdCr. Balls are Pd. |
| HX-2 | Resistivity | Open | 6 μm | 1370K 13 hrs. | Hi-Purity Argon | No | | | | | Alumina spalled off substrate. Grid detached but not melted. Sample put in furnace at temperature |
| HX-29 | Test Patch | | | 1390K 11 hrs. | Air | No | | | | | Tested 5 cycles to 1250K @ 50K/min, to check adherence of film. No effect, good adherence. |
| HX-8 | Resistivity | 140Ω | 6 μm | 1370K 10 hrs. | Air | No | | | 35 Ω | | $\alpha$ = 2000μΩ/Ω/K, Pt lead spot welded and cemented, failed after 2 cycles. |
| HX-24 | Test Patch | .52Ω | 5 μm | 1370K 2 hrs. | Bottled Argon | No | | | .55 Ω | Hi-Resis. $Cr_2O_3$<1 μm | Rough uniform surface. Very few balls on $Al_2O_3$ near PdCr. |
| HX-9 | Resistivity | 165Ω | 6 μm | 1250K 10 hrs. | Air | No | | | .56 Ω | 2 μm | $\alpha$ = 1600μΩ/Ω/K. Total drift -22,500 μΩ/Ω. Drift rate final 20 hrs. 227 μΩ/Ω/hr. |
| HX-10 | Resistivity | 144Ω | 6.2 μm | 1370K 5 hrs. | Bottled Argon | No | | | 111 Ω | Light Green 1-1.5 μm | Resis. dropped to 79 after 1st cycle in air. Sample failed (open) after 2 hr. of drift. |
| HX-23 | Test Patch | | 2.8 μm | 1370K 2 hrs. 1270K 48 hrs. | Hi-Purity Argon | No | | | .75 Ω | Hi-Resis. $Cr_2O_3$(<1μm) + $Al_2O_3$? | 1/8" strip grit-blasted @ P&W. Sent to Probe. |
| HX-27 | Test Patch | | 5 μm | | | 1 μm | 1250K 8 hrs. | Air | | | Film looks good, Al on sputtered film. |
| HX-5 | Resistivity | 122Ω | 6.5 μm | Same as HX-23 | | .5 μm | 1250K | Air | | | Grid open after oxidation. Protrusions growing out edge of film (Al sputtered on after 1st H.T. treatment. |
| HX-3 | Resistivity | 143Ω | 6 μm | | | .25 μm | 850K 24 hrs. 1250K 24 hr. | Air Hi-Purity Argon | | | Grid open after heat-treatment. Reaction at edges film, though not as bad as HX-5. (At sputtered on before H.T. heat treatments produced flat, 1/2 round melts). |

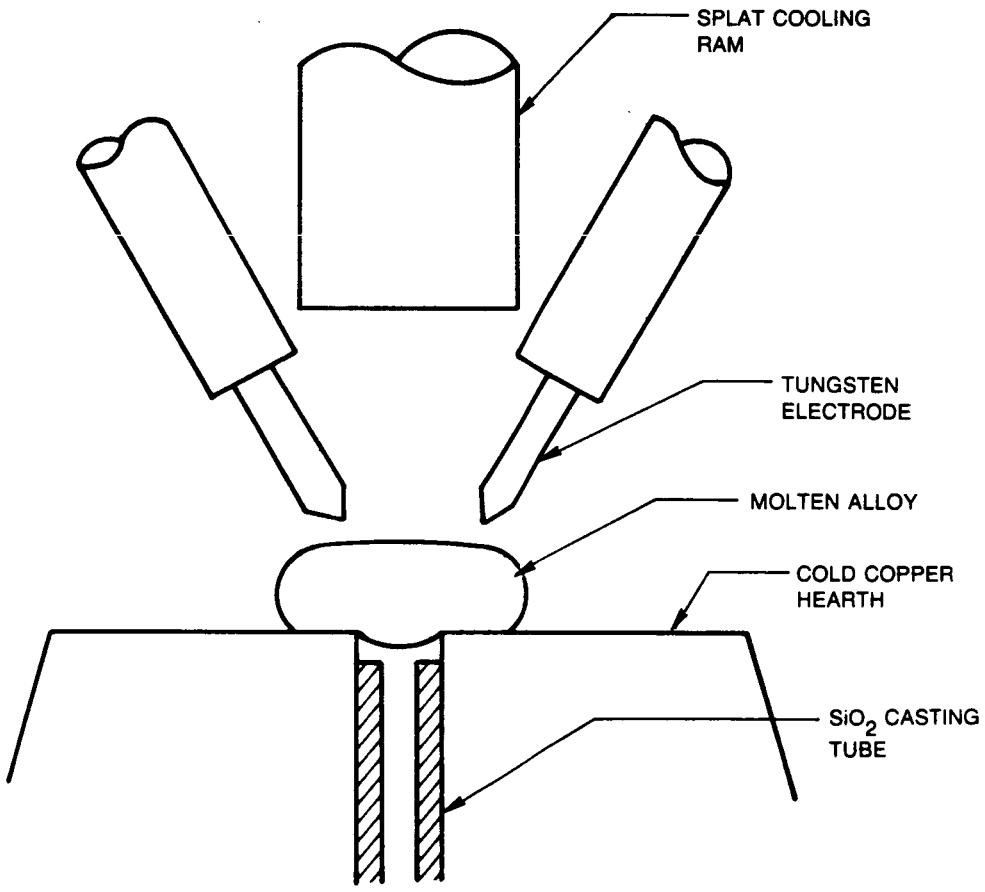


**Figure 4.1.1. Tri-arc melter showing position of splat cooling Ram and drop-casting tube.**

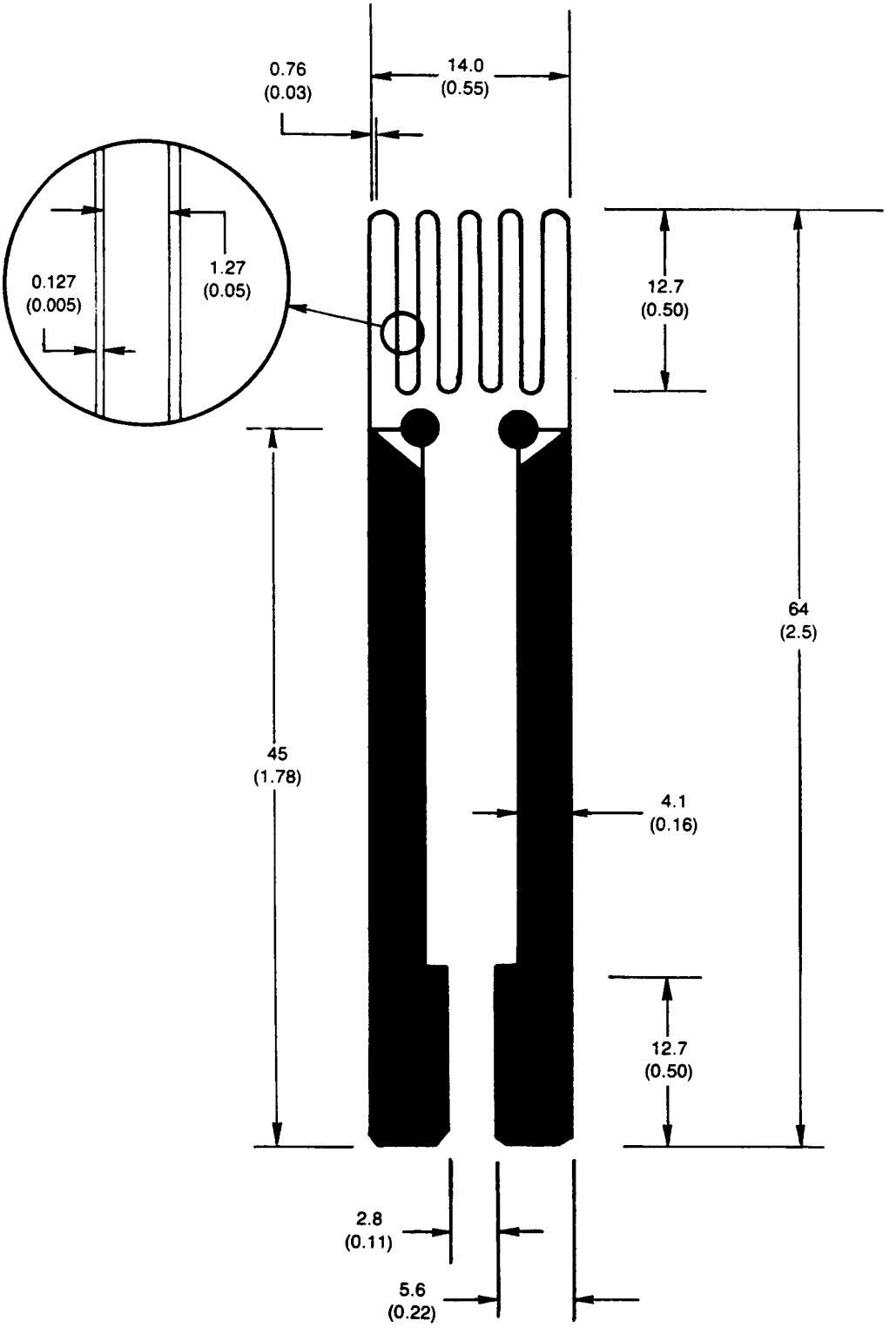


ALL DIMENSIONS IN mm (inches)

**Figure 4.1.2. Configuration of sputtered strain gage.**

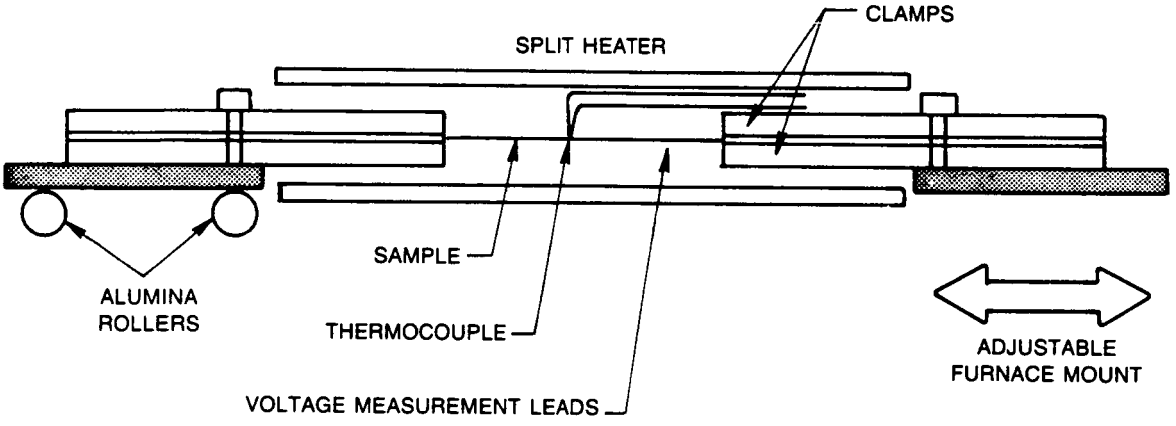


**Figure 4.2.1. High speed thermal cycle resistance measurement apparatus.**

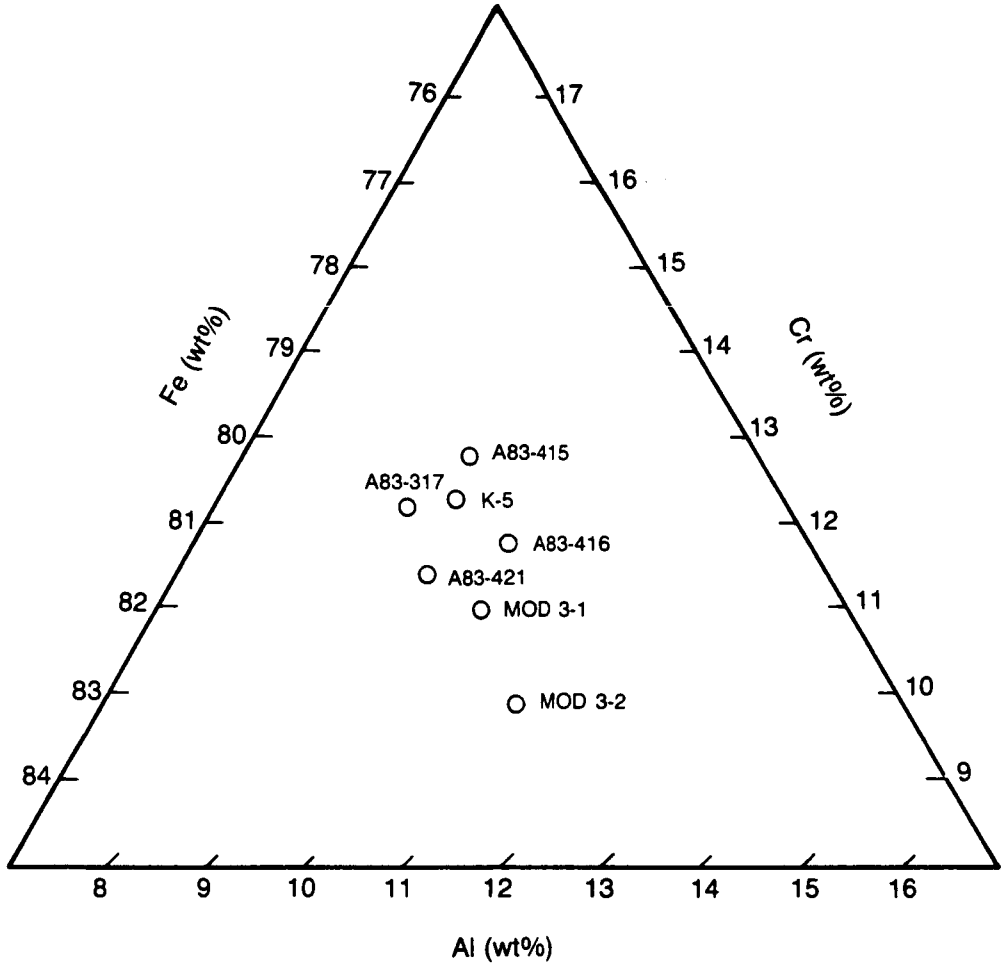


**Figure 5.2.1. Compositional variations in rods drop cast for resistivity measurements.**

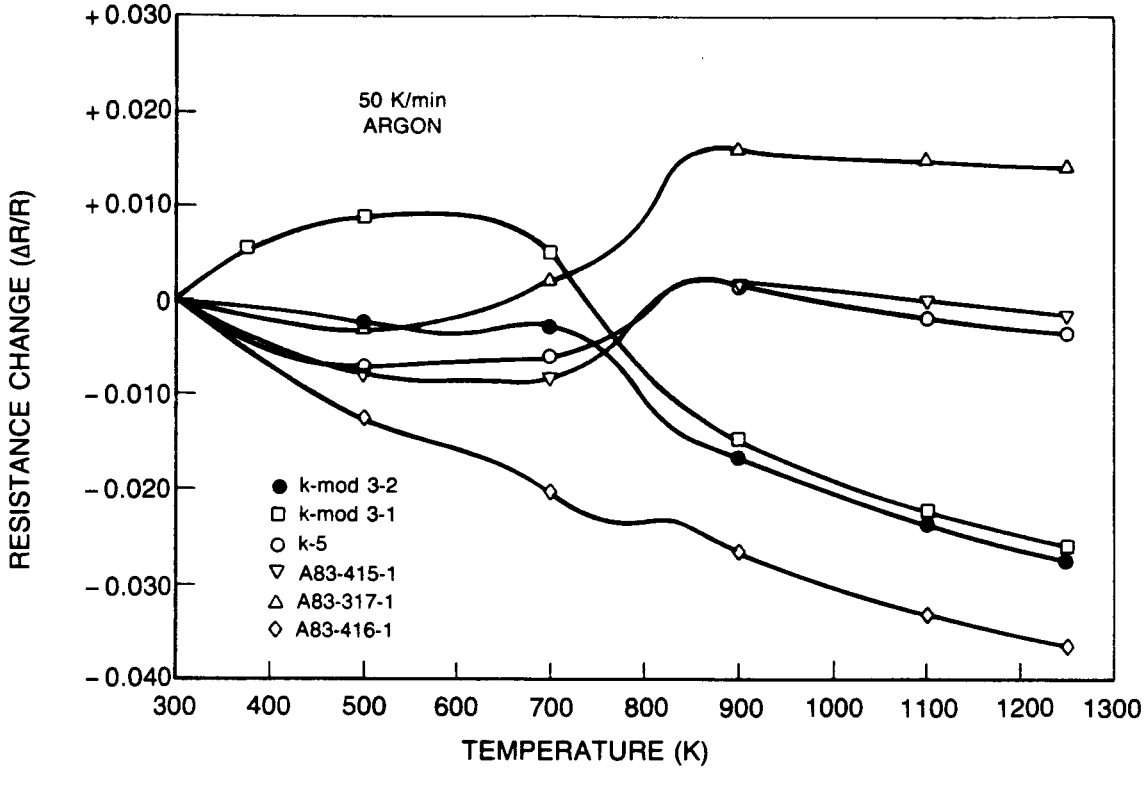


**Figure 5.2.2. Changes in resistance vs temperature of drop cast FeCrAl mod #3 rods.**

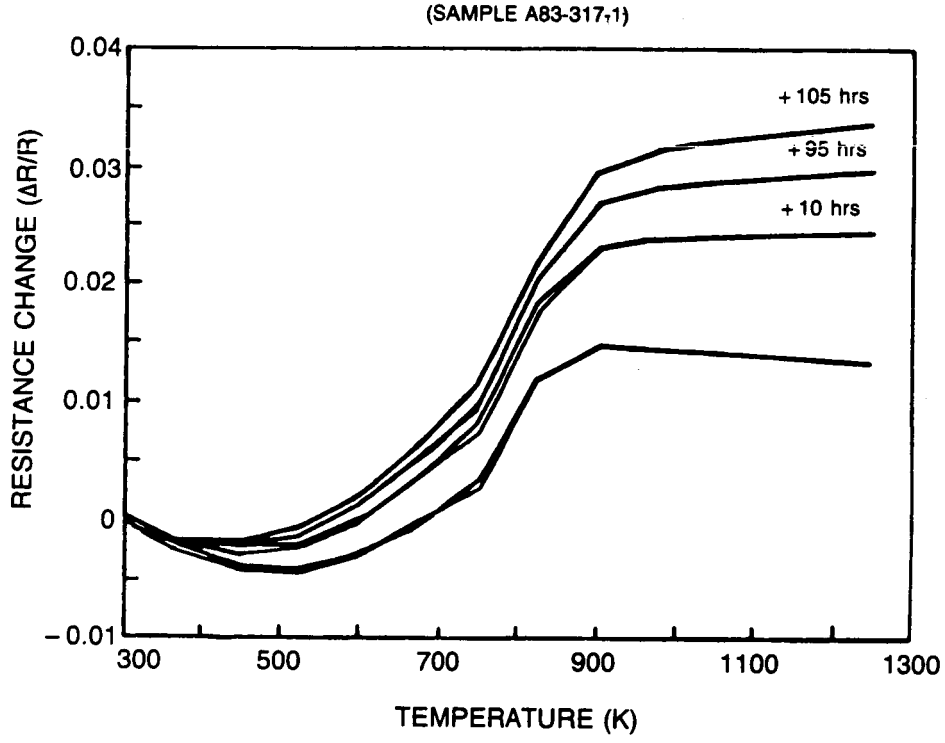


**Figure 5.2.3. Change in resistance vs temperature of FeCrAl Mod #3 after different soak times at 1250 K.**

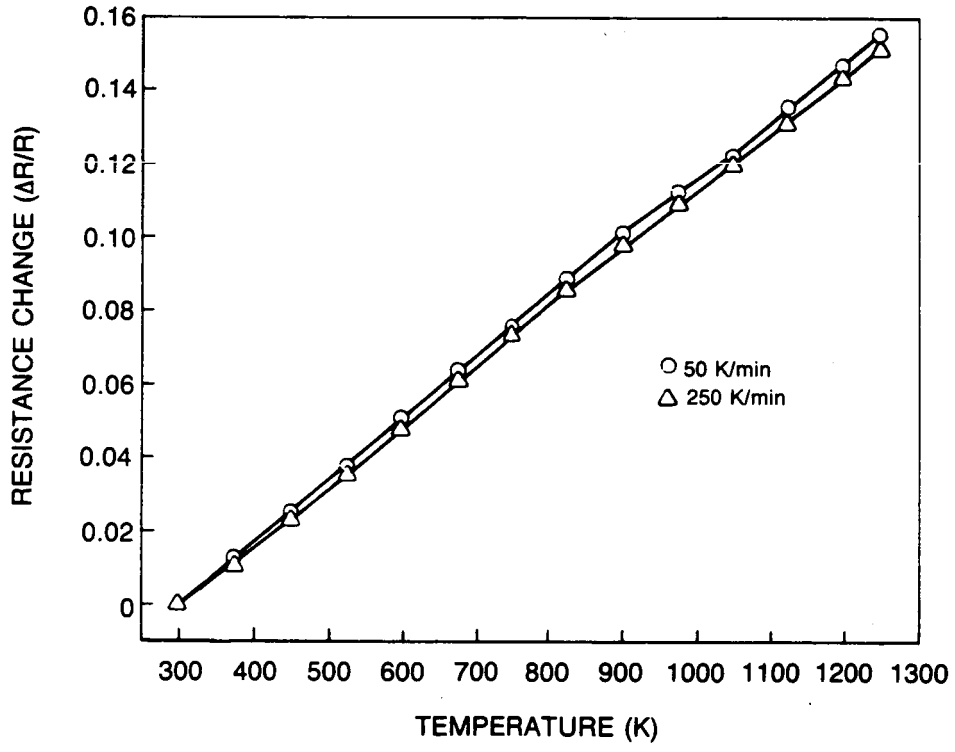


**Figure 5.3.1. Change in resistance vs temperature of Pd-13 wt% Cr at 50 and 250 K/min.**

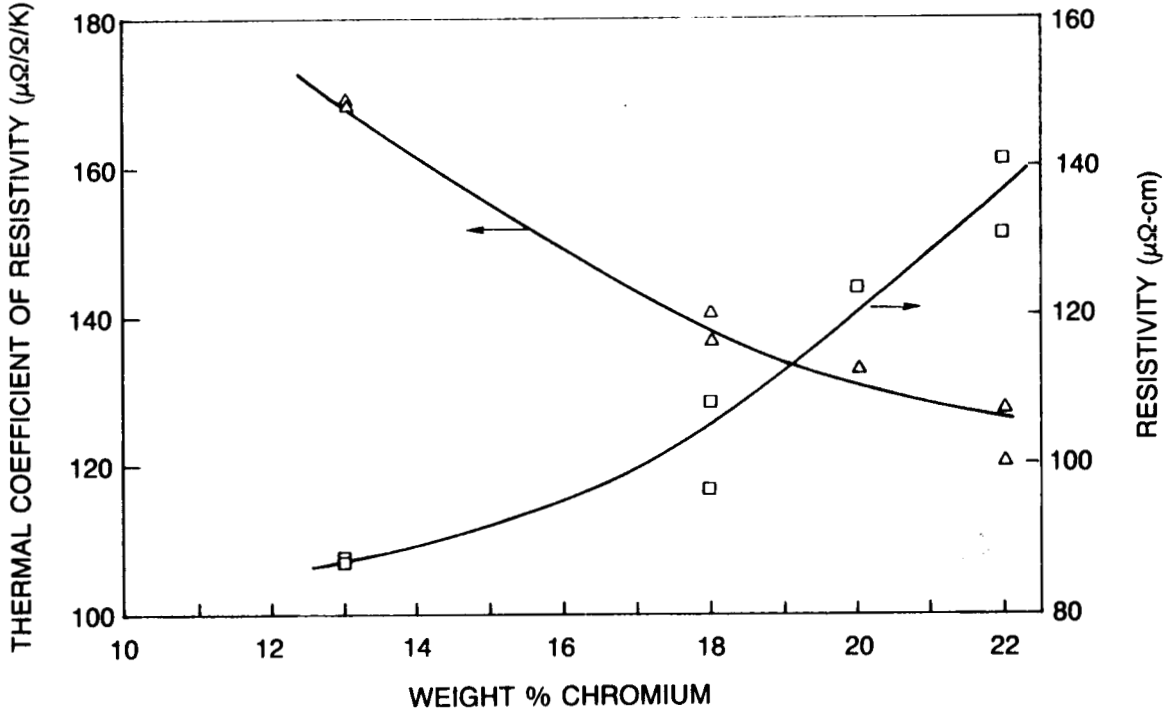


**Figure 5.3.2. Resistivity and thermal coefficient of resistivity of PdCr alloys.**

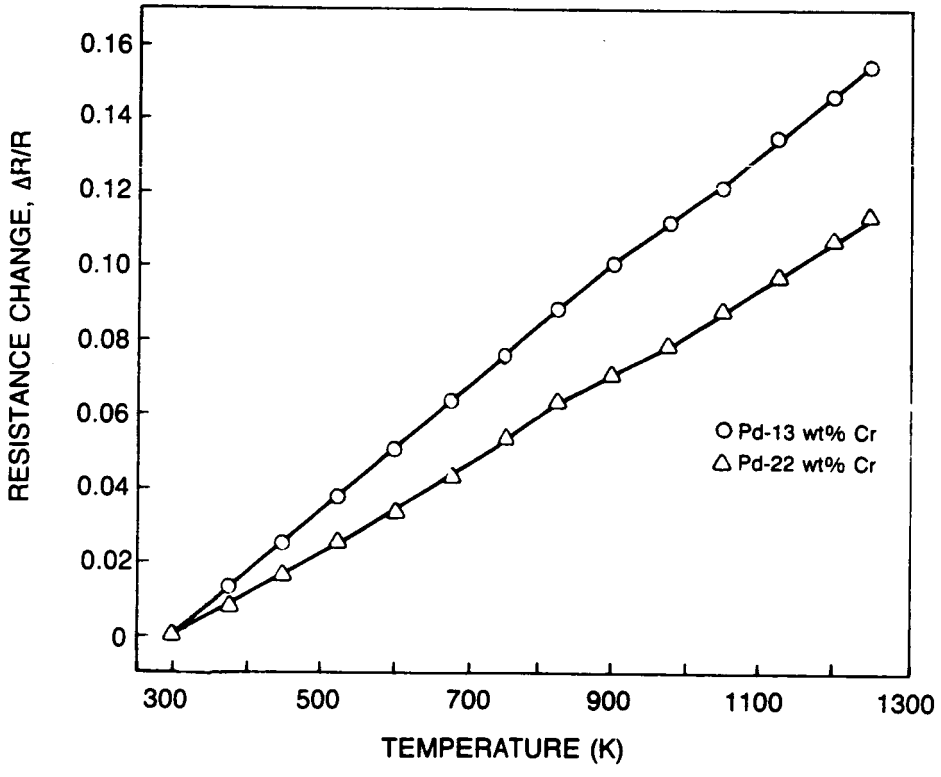


**Figure 5.3.3. Change in resistance vs temperature of PdCr alloys at 50 K/min.**

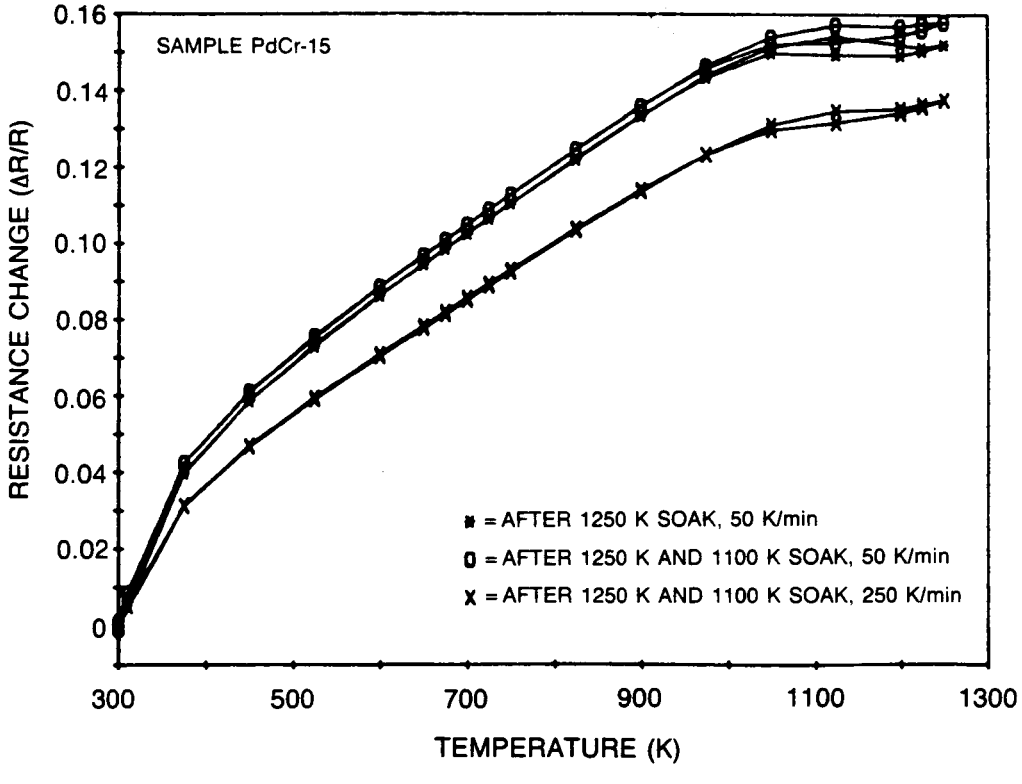


**Figure 5.3.4. Change in resistance vs temperature of Pd-18Cr-8Ta (wt%).**

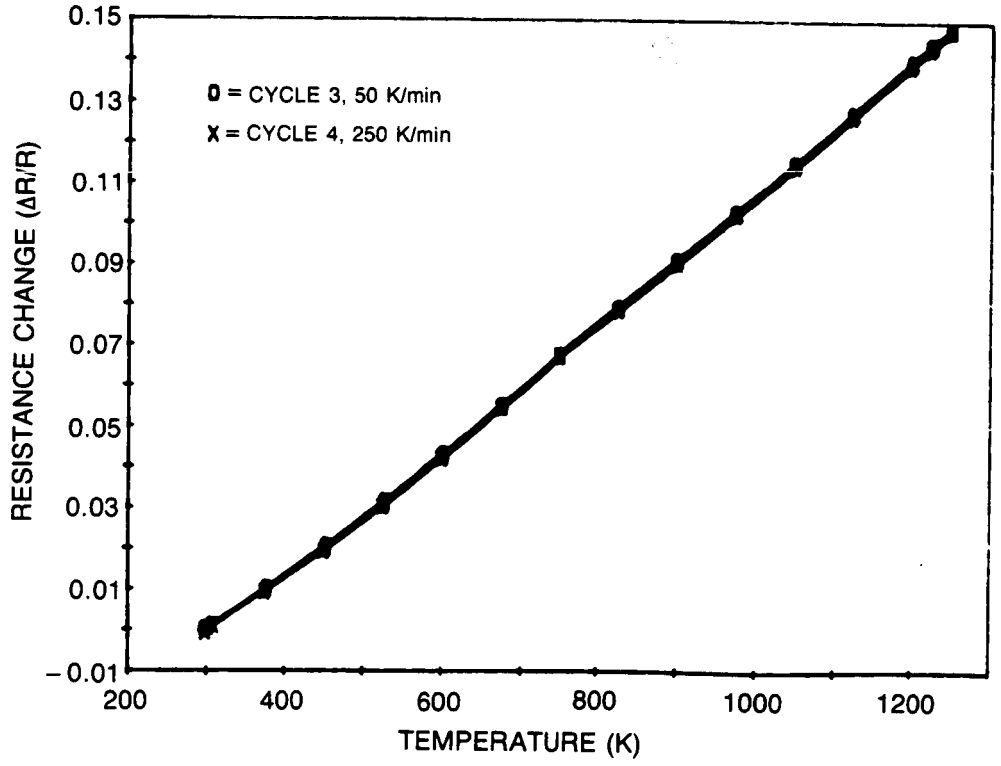


**Figure 5.3.5. Change in resistance vs temperature of Pd-16Cr-8Ni (wt%).**

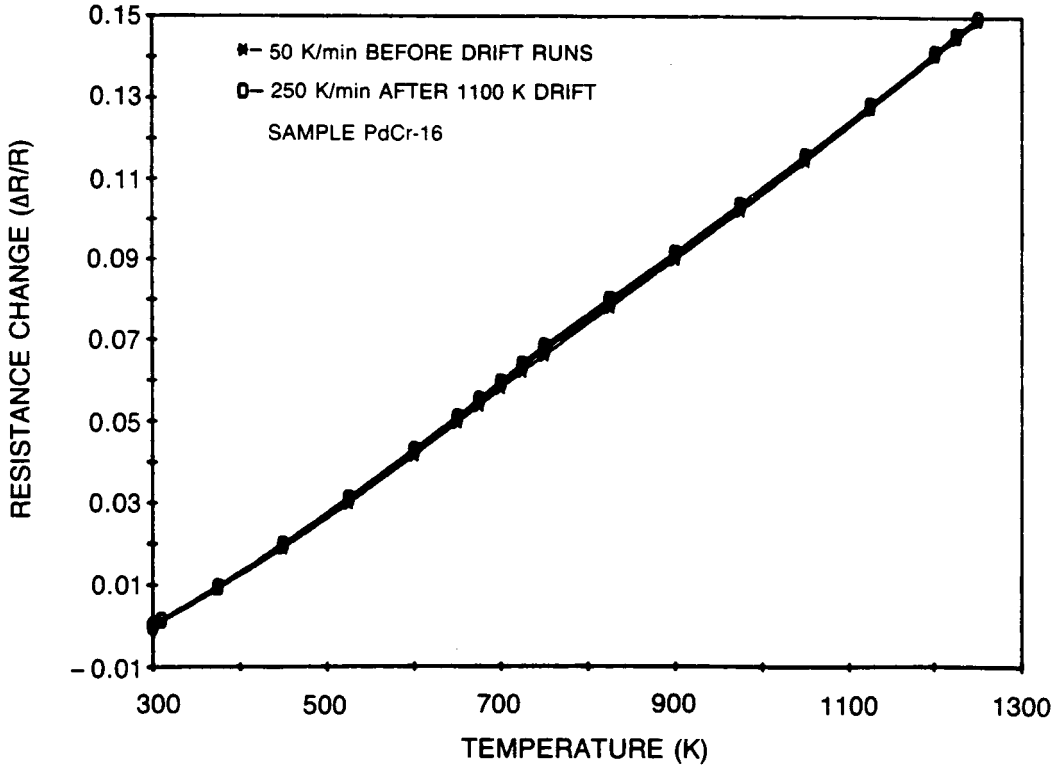


**Figure 5.3.6. Change in resistance vs temperature of Pd-16Cr-10Ni (wt%).**

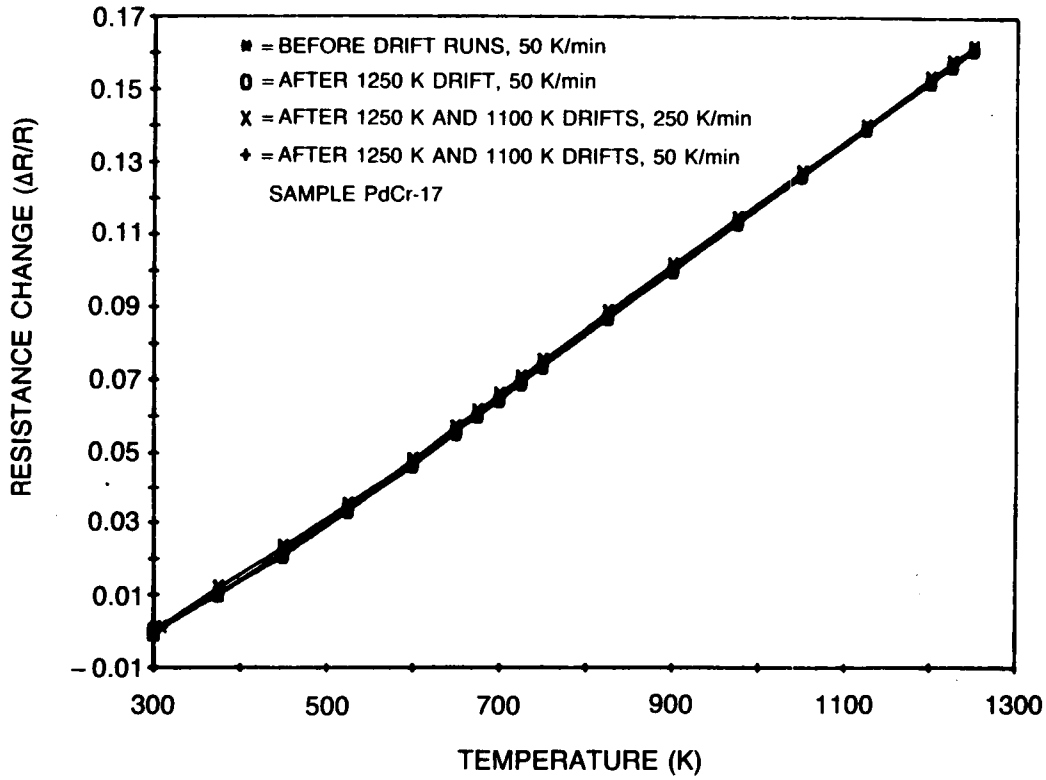


**Figure 5.3.7. Change in resistance vs temperature before and after 10 hour drift runs Pd-16Cr-8Co (wt%).**

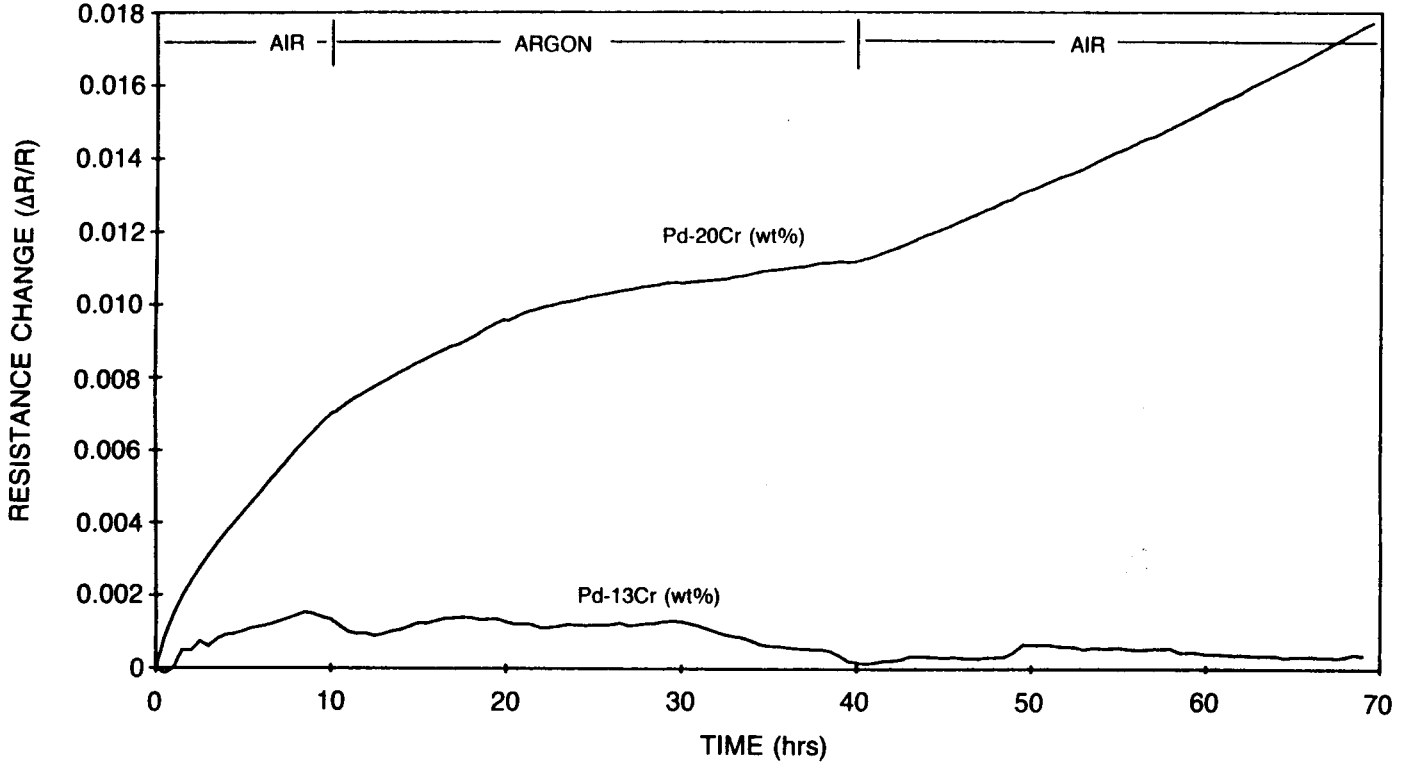


**Figure 5.3.8. Drift of Pd-20Cr (wt%) and Pd-13 Cr (wt%) at 1250 K.**

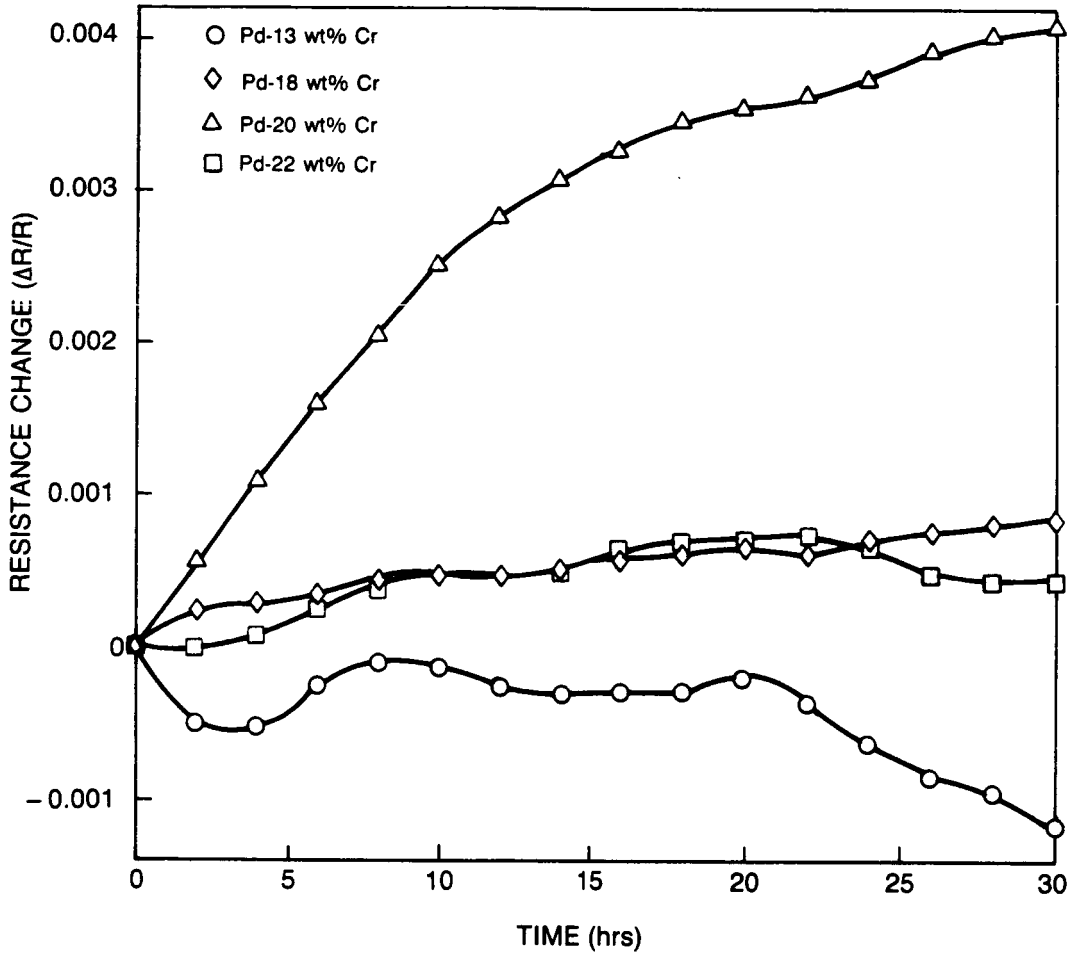


**Figure 5.3.9. Resistance drift of PdCr alloys in argon at 1250 K.**

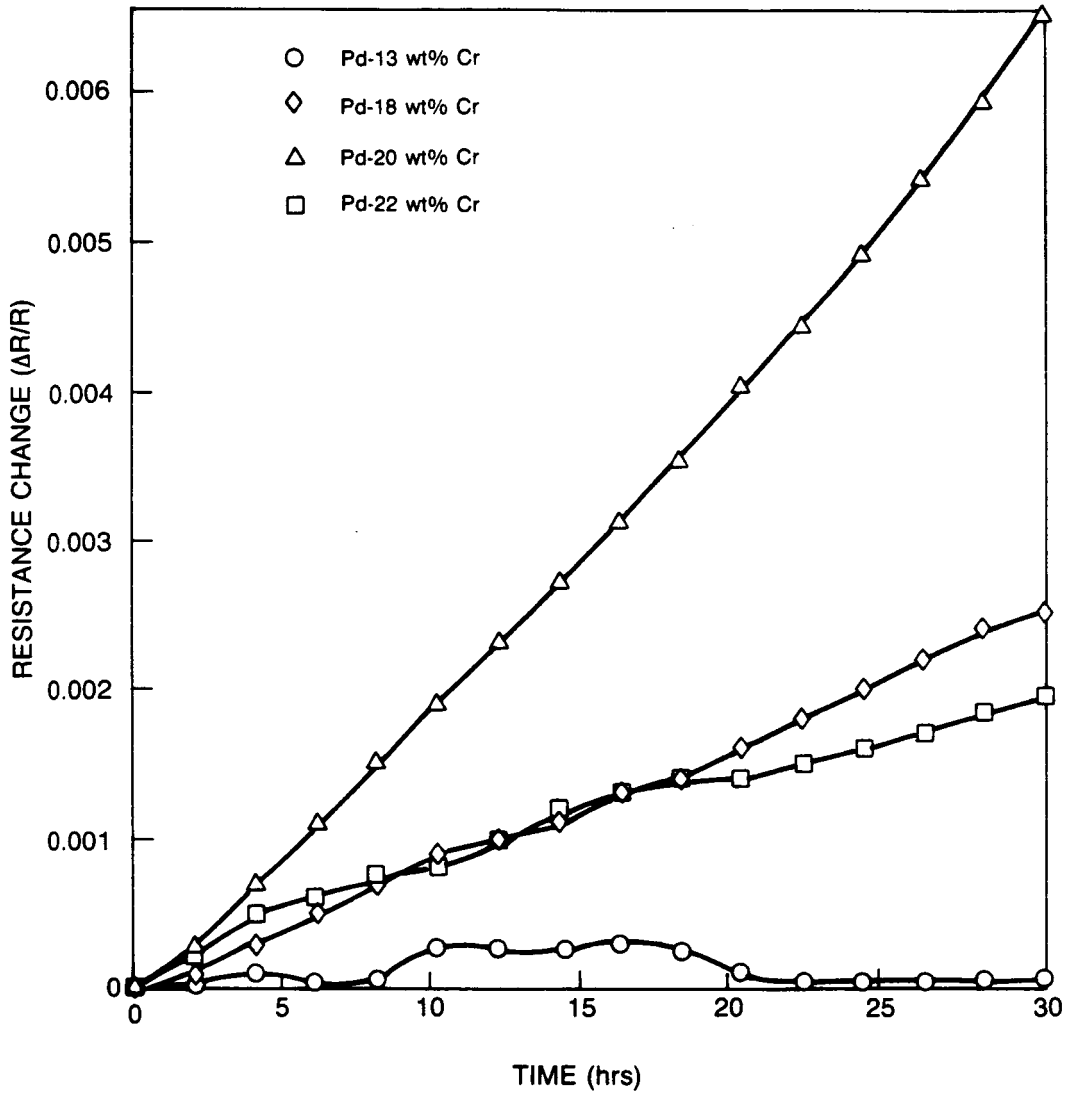


**Figure 5.3.10. Resistance drift of PdCr alloys in air at 1250 K.**

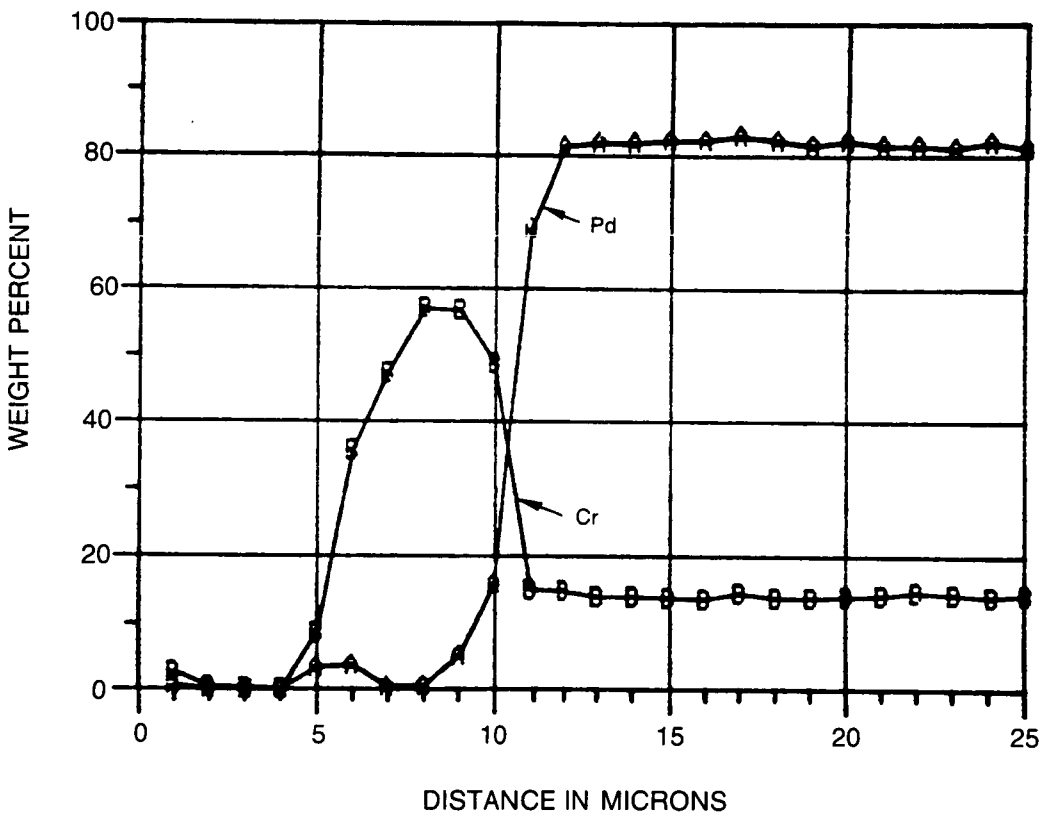


**Figure 5.3.11. Elemental composition profiles at the surface of Pd-13Cr (wt%) sample after 40 hours in air at 1250 K.**

a) SEM PICTURE

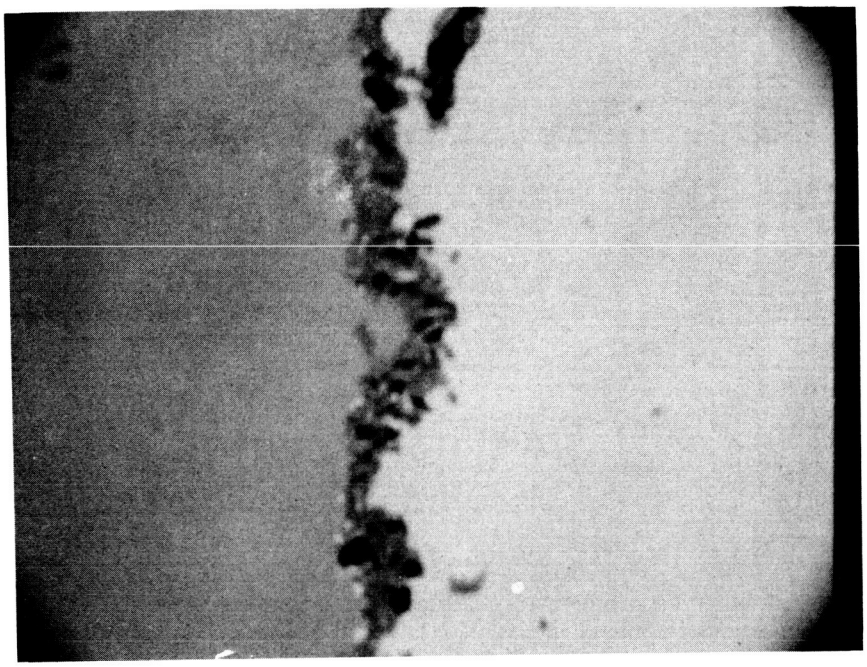

10μm

b) OXYGEN MAP

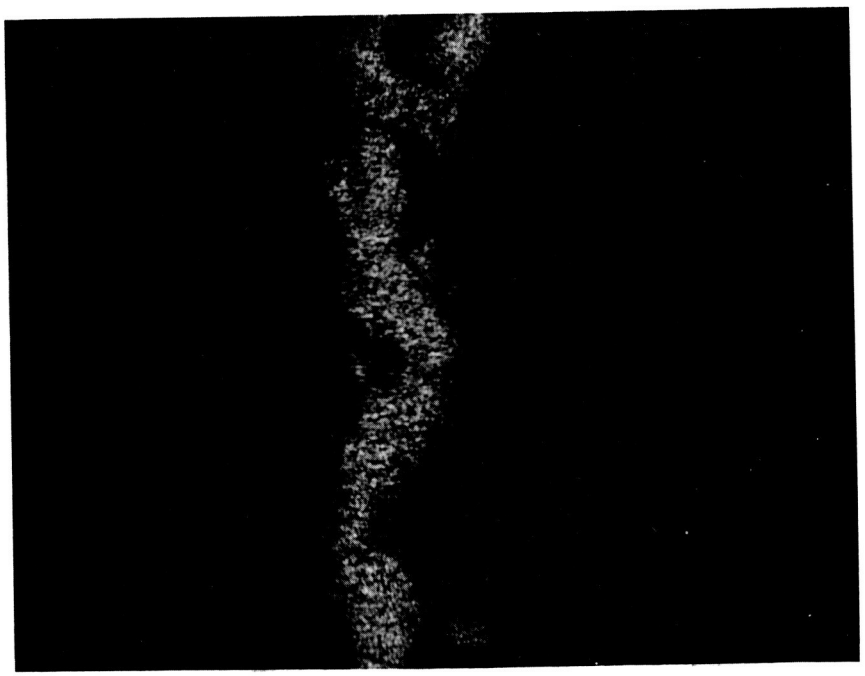

10μm

(AFTER 40 hrs IN AIR AT 1250 K)

**Figure 5.3.12. View of oxide surface film on Pd-13Cr (wt%).**

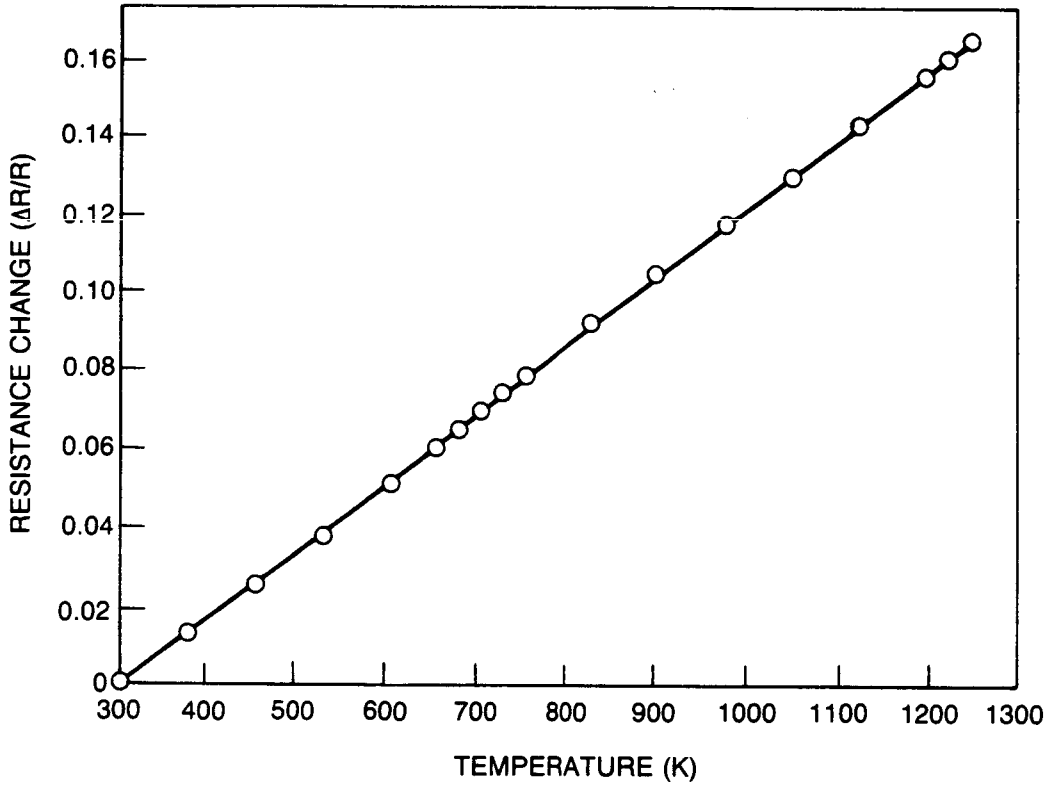


**Figure 5.3.13. Change in resistance vs temperature at 50 K/min in argon of splat cast foil Pd-13 w/o Cr (wt%).**

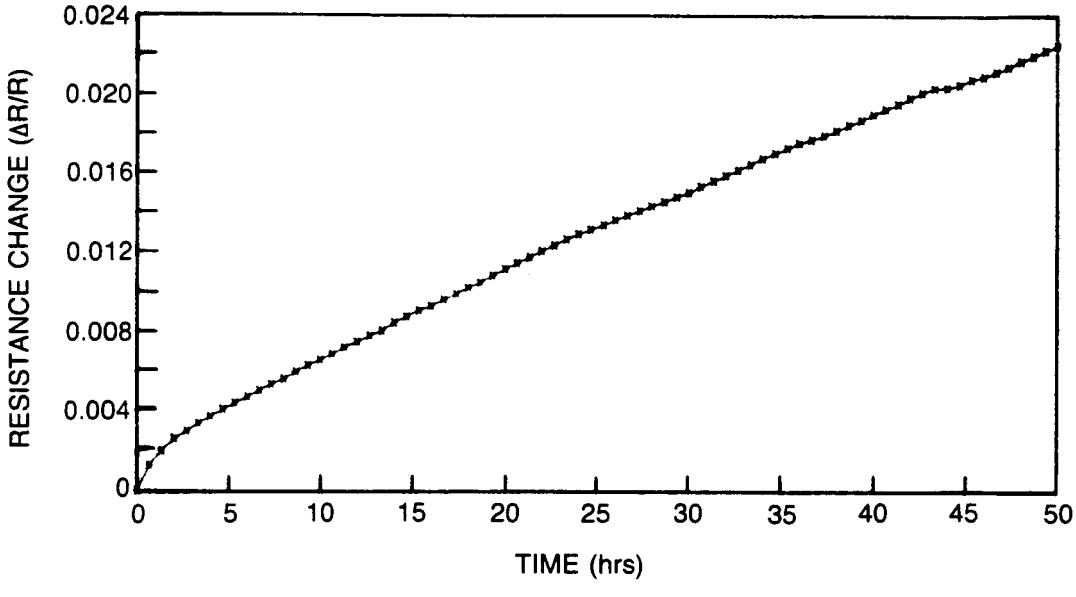


**Figure 5.3.14. Drift in resistance at 1250 K for 50 hours in air of splat cast foil Pd-13Cr (wt%).**

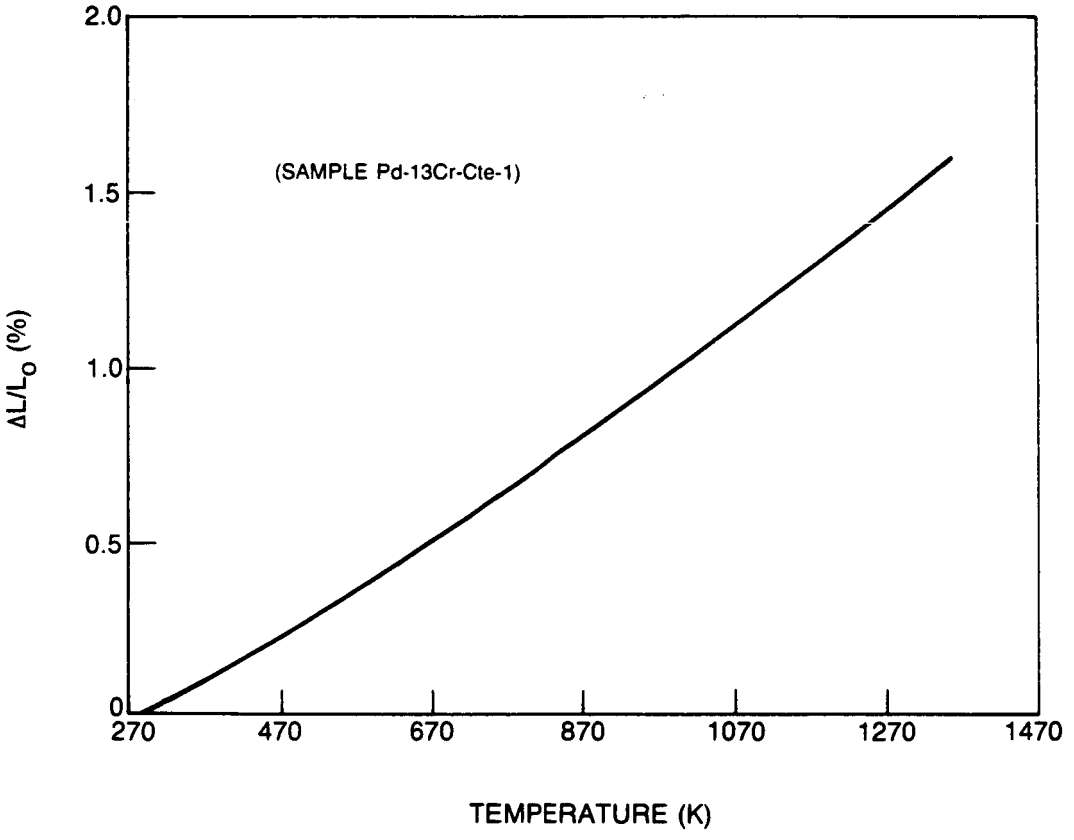


**Figure 5.4.1. Thermal expansion of Pd-13Cr (wt%) in argon.**

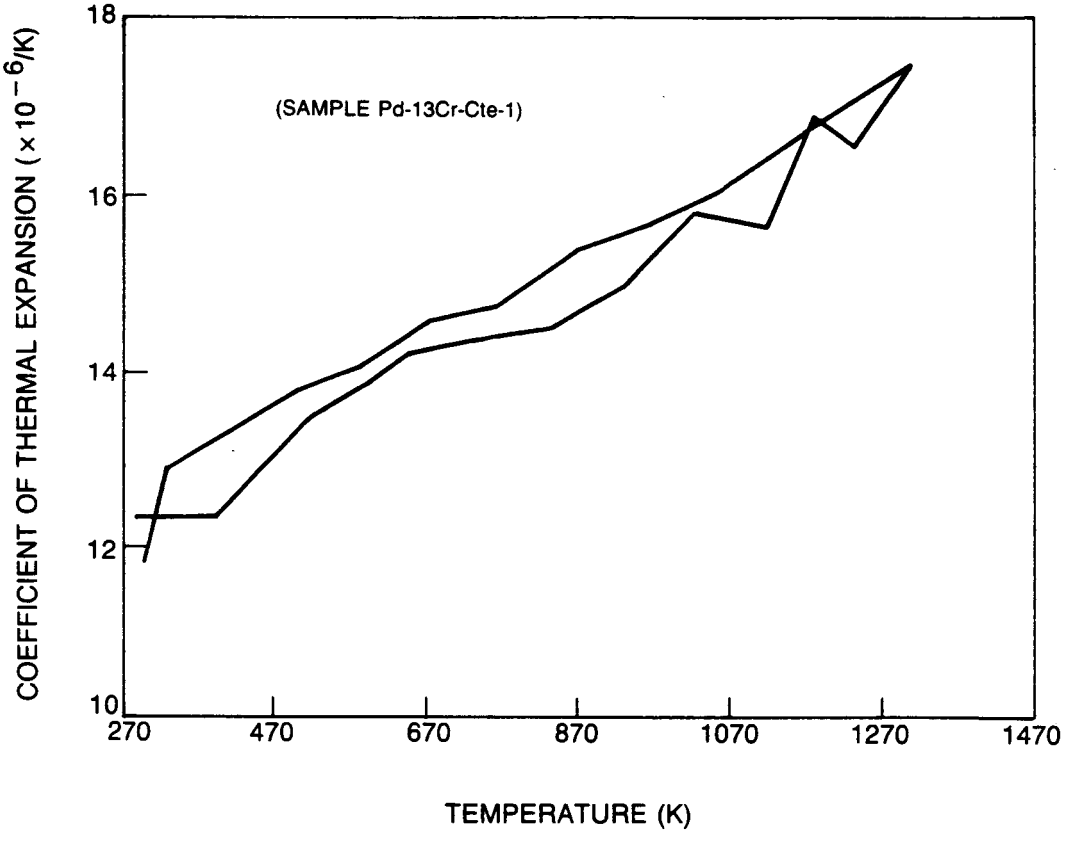


**Figure 5.4.2. Coefficient of thermal expansion of Pd-13Cr (wt%) in argon.**

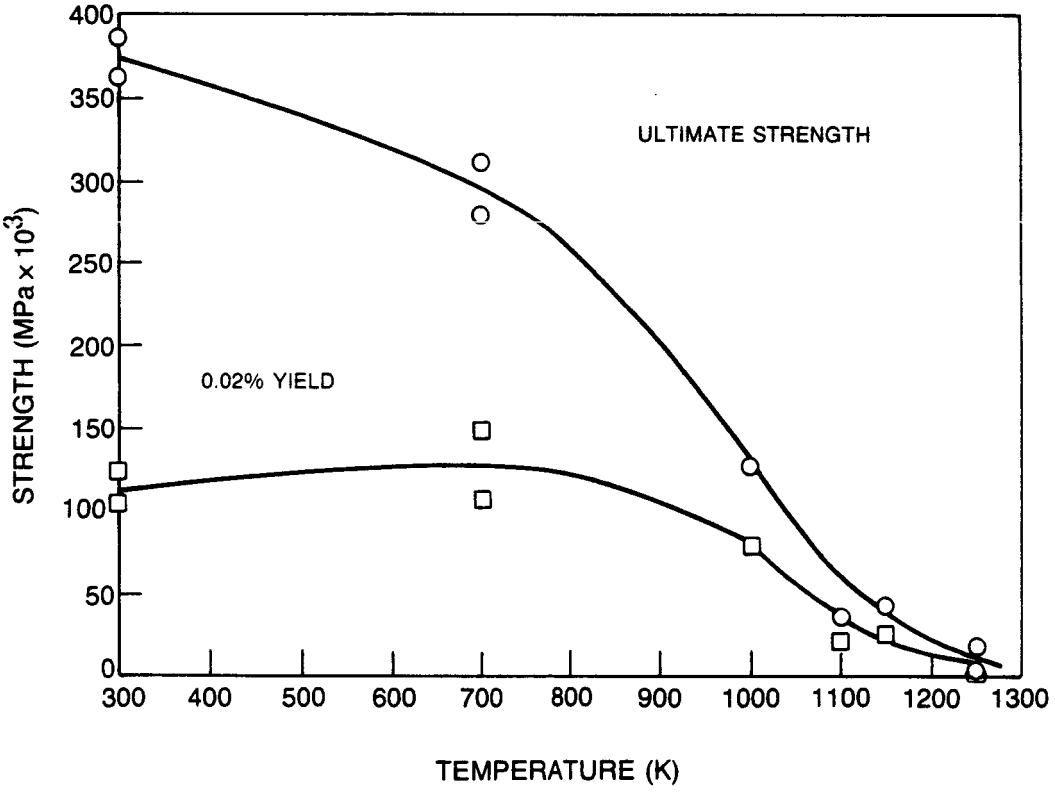


**Figure 5.4.3. Strength vs temperature of drop cast Pd-13Cr (wt%).**

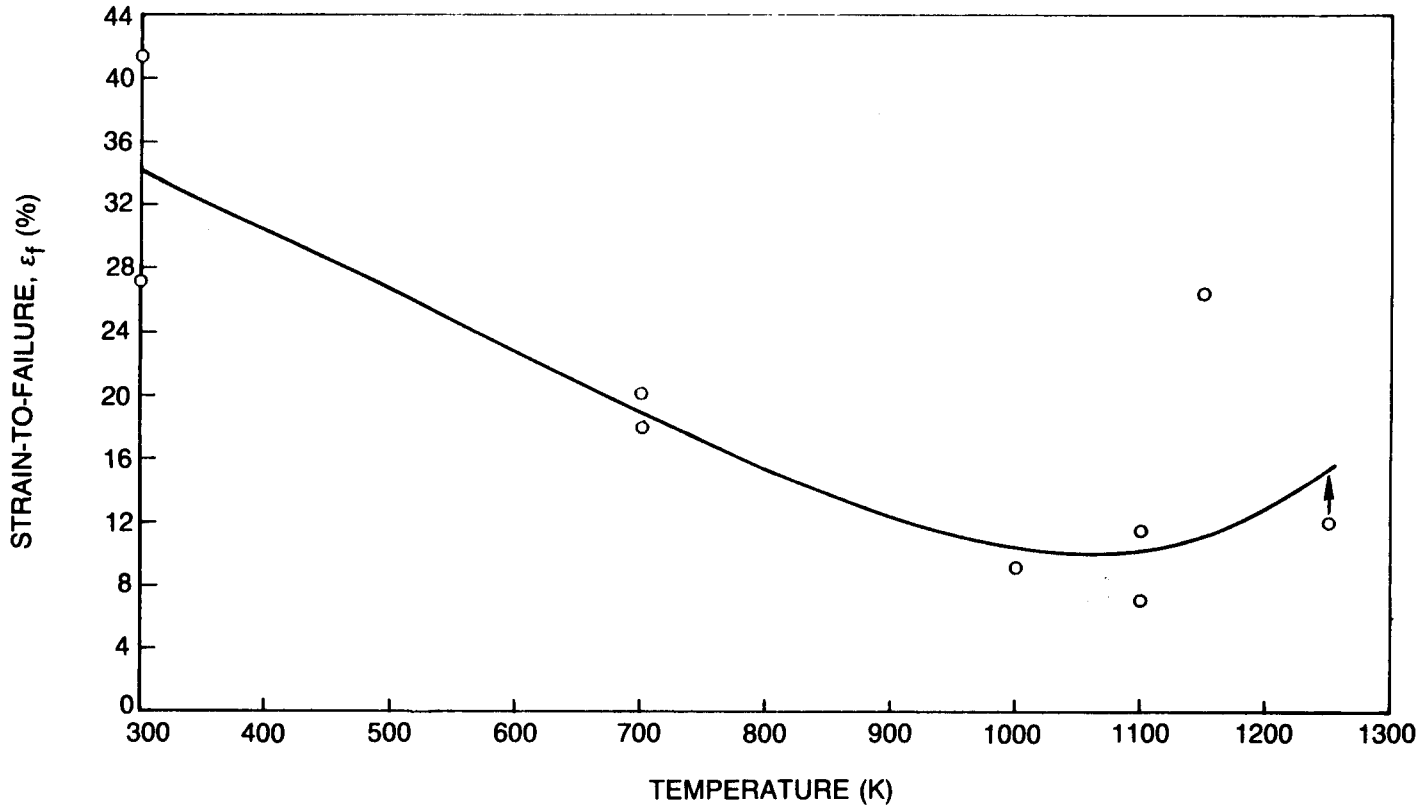


**Figure 5.4.4. Strain-to-failure vs temperature of drop cast Pd-13Cr (wt%).**

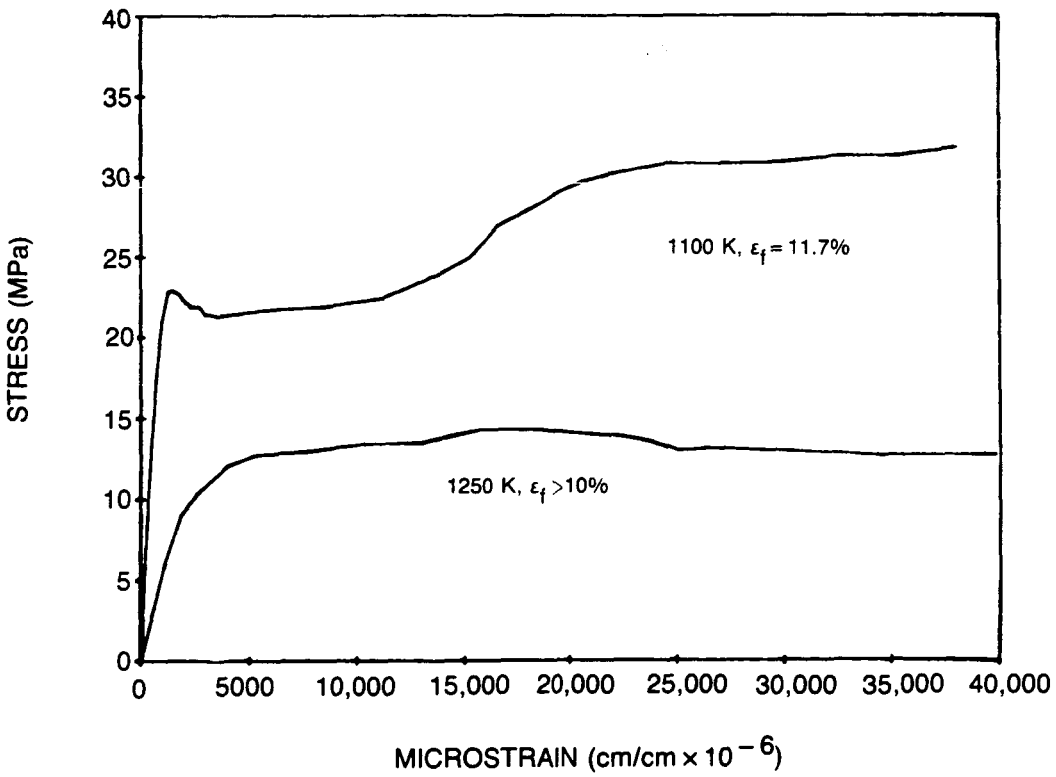


**Figure 5.4.5. High temperature stress-strain curves of drop cast Pd-13Cr (wt%).**

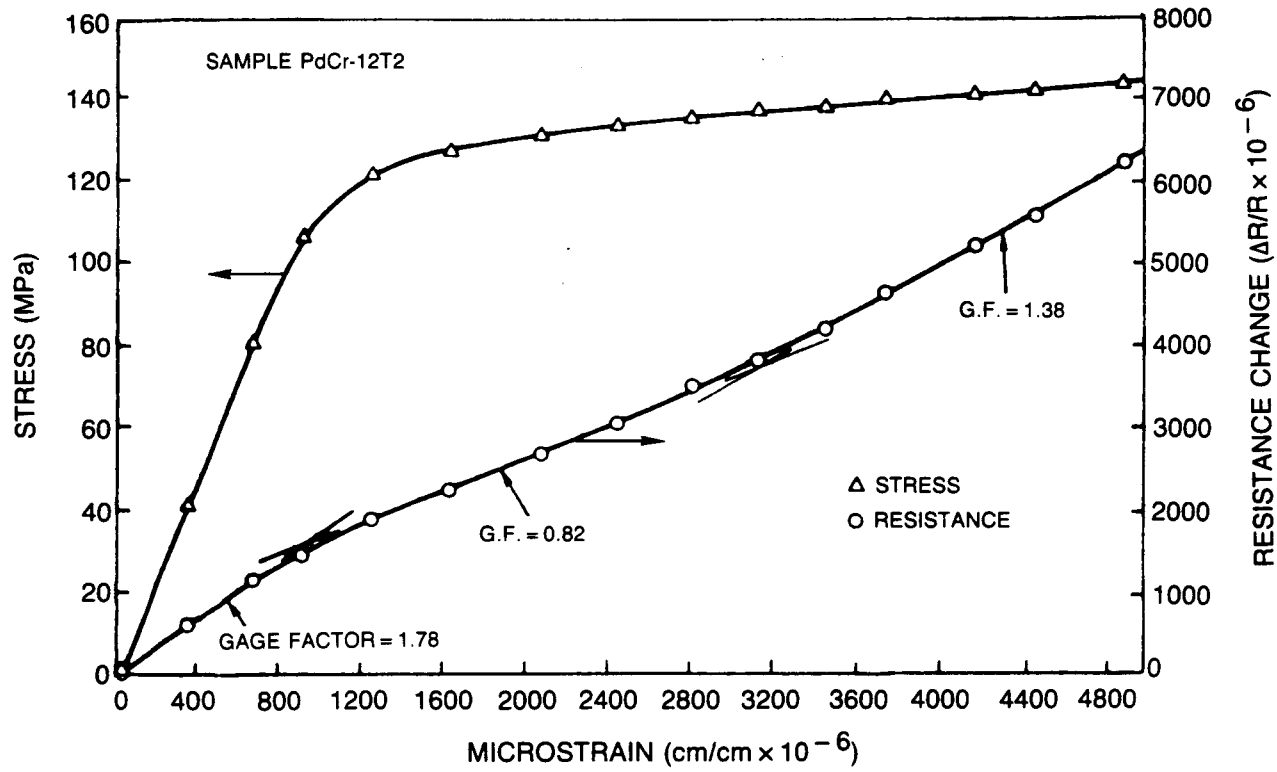


**Figure 5.4.6. Variation of resistance and stress with strain at room temperature in Pd-13Cr (wt%).**

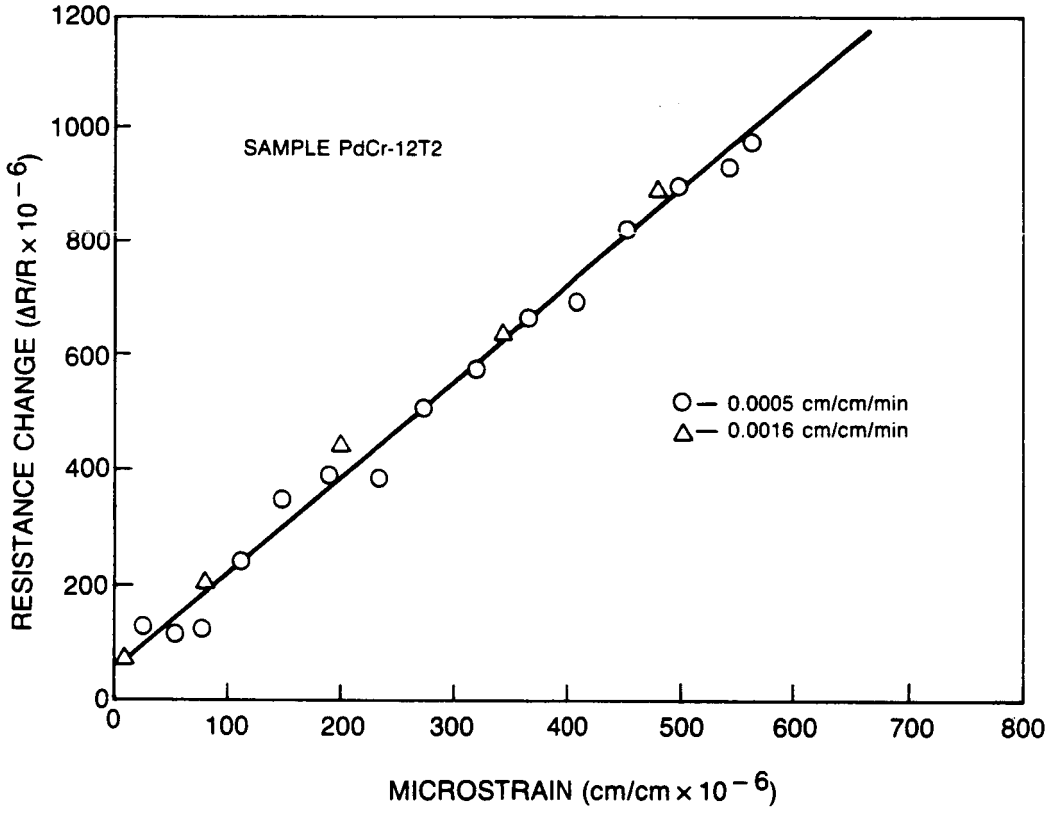


**Figure 5.4.7. Effect of strain rate on the gage factor at room temperature of Pd-13Cr (wt%).**

a) UNIFORM NODULES

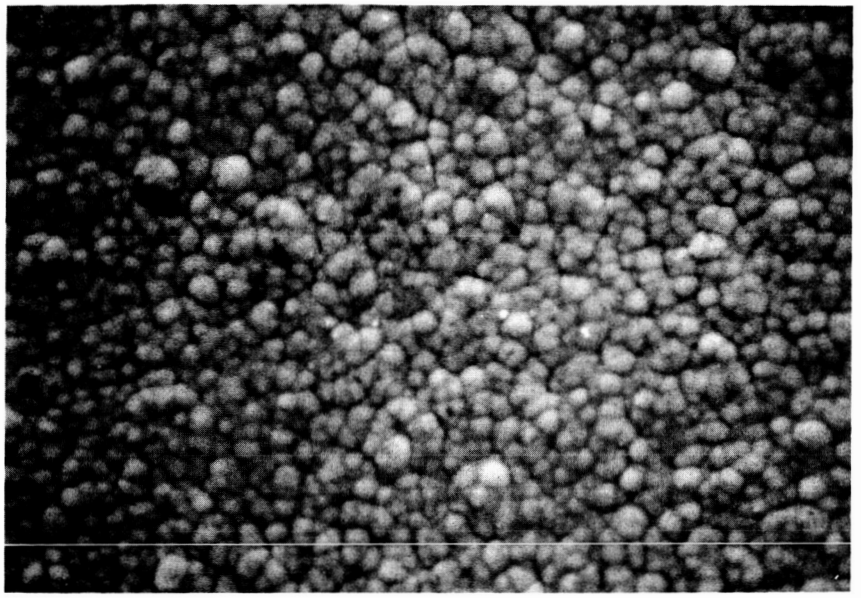

5μm

b) SOME EXAGGERATED NODULES

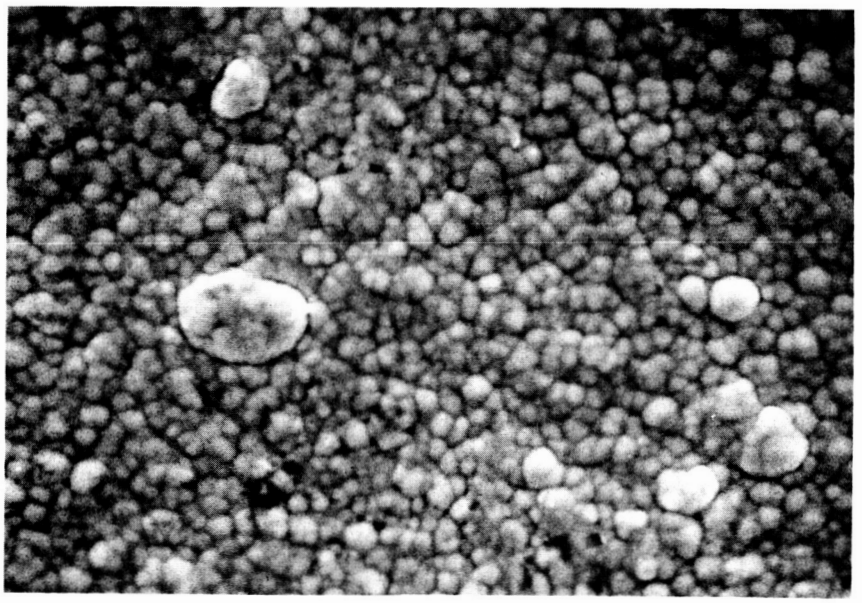

5μm

**Figure 5.5.1. As-sputtered Pd-13Cr (wt%) on coated Hast-X.**

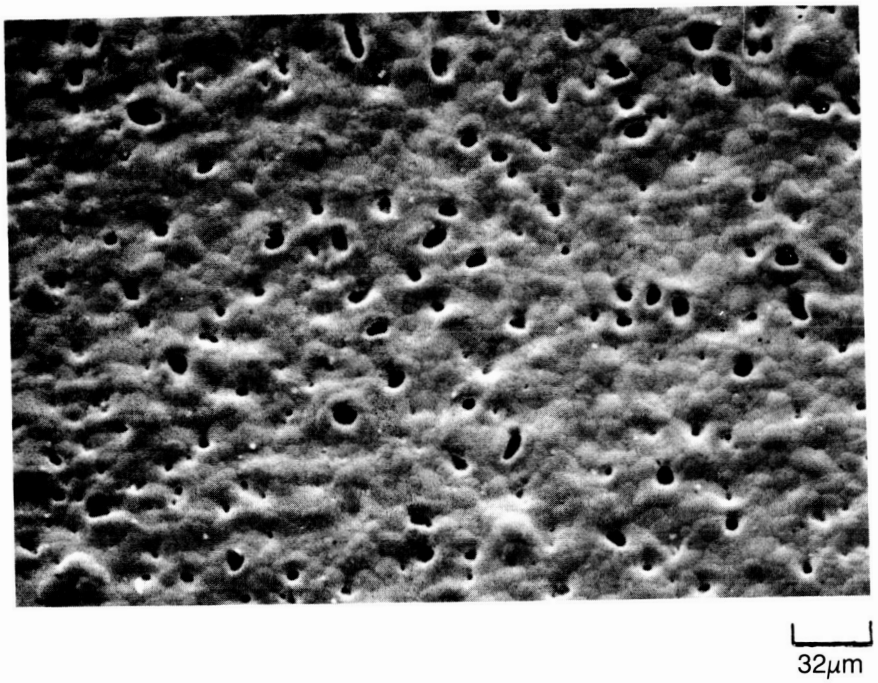


**Figure 5.5.2. Holes in sputtered PdCr films after recrystallization.**

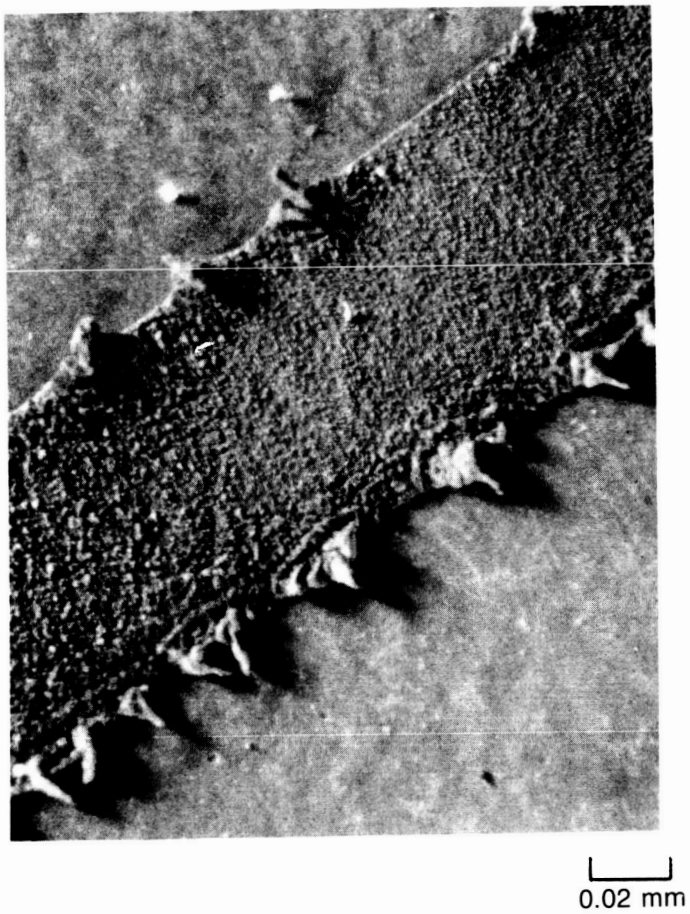


**Figure 5.5.3. Edge protrusions on PdCr grid after oxidation of 0.5$\mu$m Al overcoat (sample HX-5).**

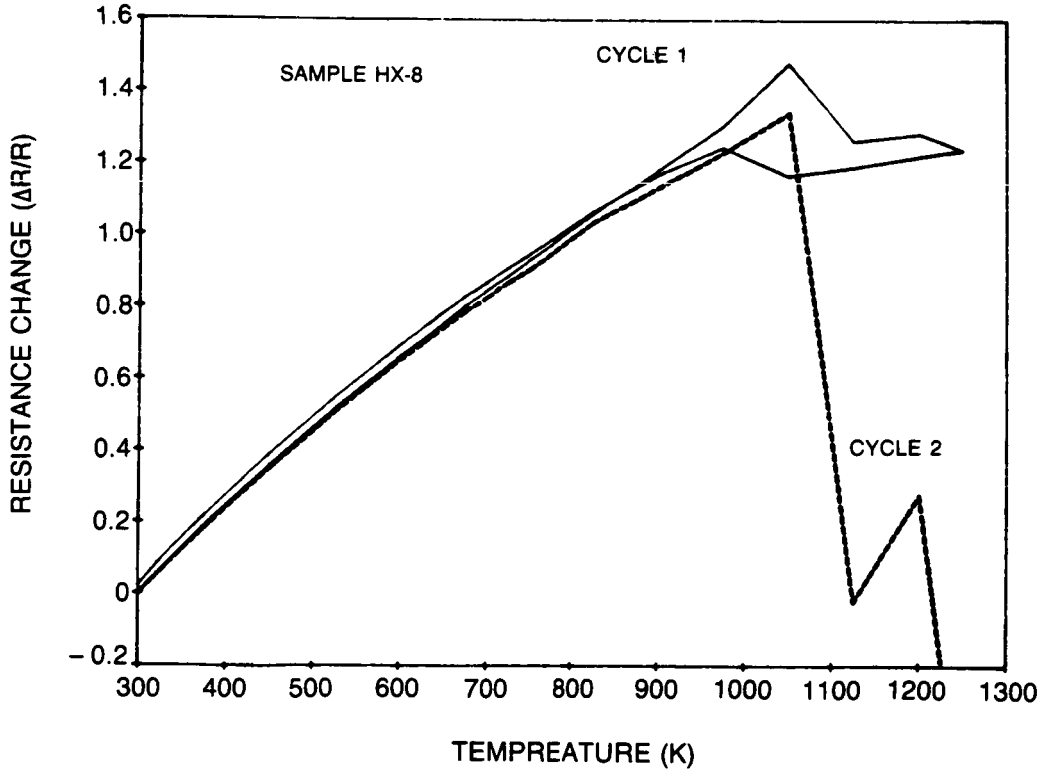


**Figure 5.6.1. Resistance vs temperature for sputtered Pd-13Cr (wt%) pretreated 10 hrs in air at 1370 K.**

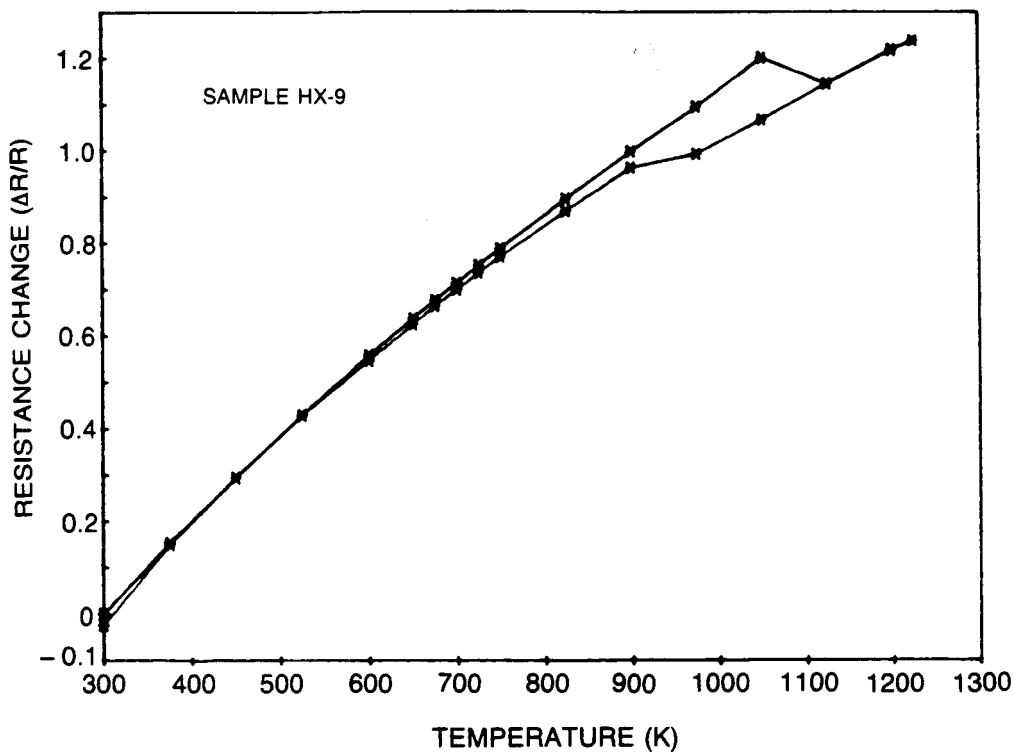


**Figure 5.6.2. Change in resistance vs temperature at 50 K/min in air Pd-13Cr (wt%) after pretreated 1250 K 10 hrs in air.**

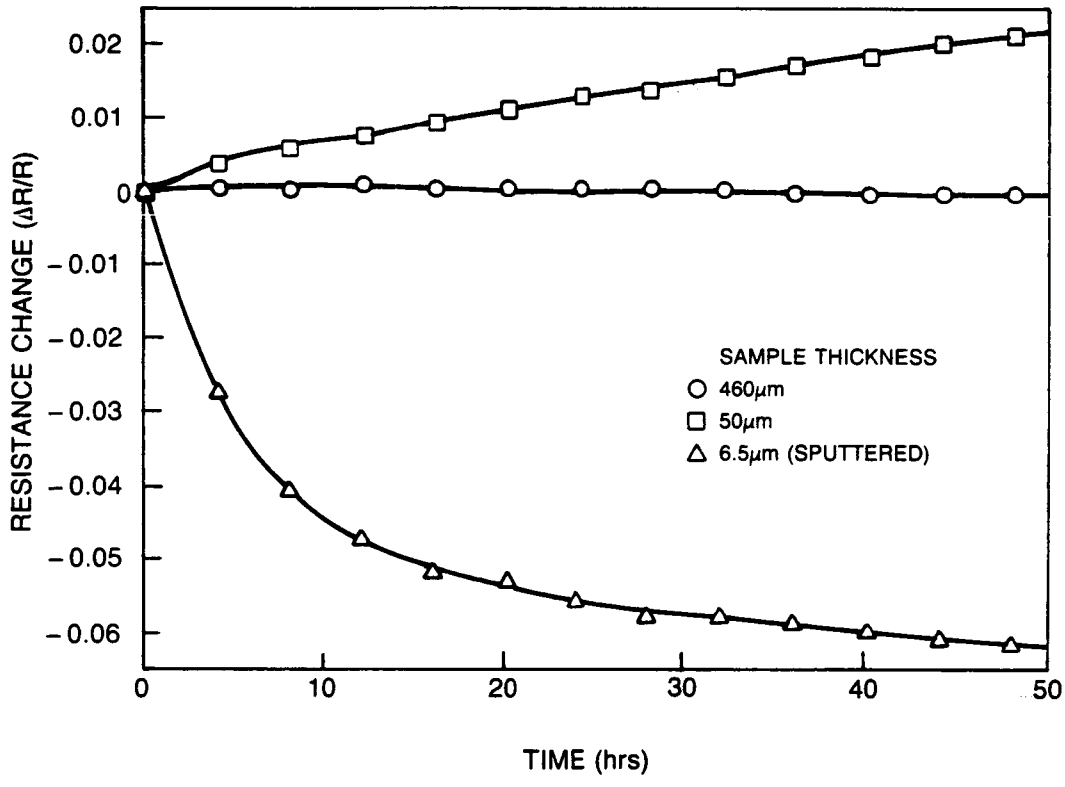


**Figure 5.6.3. Effect of sample thickness on drift in resistance of Pd-13Cr (wt%) in air at 1250 K.**

NASA
National Aeronautics and Space Administration

# Report Documentation Page

| 1. Report No. | 2. Government Accession No. | 3. Recipient's Catalog No. |
|---|---|---|
| CR 180811 | | |

**4. Title and Subtitle**
High Temperature Static Strain Gage Development Contract (Interim Report, Tasks 1 and 2)

**5. Report Date**
August 1986

**6. Performing Organization Code**

**7. Author(s)**
C. O. Hulse, R. S. Bailey, H. P. Grant and J.S. Przybyszewski

**8. Performing Organization Report No.**
R87-916527-1

**10. Work Unit No.**
533-04-11

**9. Performing Organization Name and Address**
United Technologies Corporation
United Technologies Research Center
East Hartford, CT 06108

**11. Contract or Grant No.**
NASA NAS 3-23722

**13. Type of Report and Period Covered**
Interim

**12. Sponsoring Agency Name and Address**
Project Manager: W. Kim
National Aeronautics and Space Administration
Lewis Research Center
2100 Brookpark Road, Cleveland, Ohio 44135

**14. Sponsoring Agency Code**

**15. Supplementary Notes**

ORIGINAL PAGE IS
OF POOR QUALITY

**16. Abstract**

Interim results are presented from a program to develop static strain gages for use on the blades and vanes of running, test-stand gas turbine engines with goals of a 3 mm x 3 mm gage area and total errors of less than 10% of ± 2,000 microstrain after 50 hours at 1250 K. The basic concepts which directed these efforts were that successful sensor alloys must be single phase and contain a high concentration of electron scattering alloying elements which would remain in complete solid solution over the full temperature range of interest. None of the alloying elements added to Fe-10.6Cr-11.9Al or to Pd-13Cr (in wt. percent) appeared to provide improved resistances to oxidation or to lower the thermal sensitivity of resistance. Studies on FeCrAl alloys were discontinued when it was discovered that extended exposures to 1250 K in air resulted in gradual shifts in the temperature/resistance curves toward high resistivity. The detrimental effects of oxidation on resistance properties increased significantly when the PdCr alloy was prepared as a 6.5 μm thick sputtered film compared with thicker samples prepared by drop casting. Problems were also encountered in preventing electrical leakage through the grown and sputtered alumina insulation layer to the Hast-X substrate. Attempts to retard oxidation attack by applying thin overcoats of Al which were subsequently oxidized were not successful, primarily because the impervious scale which formed on the aluminum prevented complete oxidation. Additional efforts to develop impervious overcoats are required.

**17. Key Words (Suggested by Author(s))**
- Strain Gages
- Elevated Temperatures
- Static Strain
- Electrical Resistance
- Sputtered

for general release August 1987.

| 19. Security Classif. (of this report) | 20. Security Classif. (of this page) | 21. No of pages | 22. Price* |
|---|---|---|---|
| Unclassified | Unclassified | 80 | |

NASA FORM 1626 OCT 86

*For sale by the National Technical Information Service, Springfield, Virginia 22161